Inorganics **2014**, *2*, 620-648; doi:10.3390/inorganics2040620

OPEN ACCESS

inorganics

ISSN 2304-6740

www.mdpi.com/journal/inorganics

Article

Experimental and Theoretical Studies of the Factors Affecting the Cycloplatination of the Chiral Ferrocenylaldimine (*S*$_C$)-[(η^5-C$_5$H$_5$)Fe{(η^5-C$_5$H$_4$)–C(H)=N–CH(Me)(C$_6$H$_5$)}]

Concepción López [1,*], Ramón Bosque [1,*], Marta Pujol [1], Jonathan Simó [1], Eila Sevilla [1], Mercè Font-Bardía [2], Ramon Messeguer [3] and Carme Calvis [3]

[1] Departament de Química Inorgánica, Facultat de Química, Universitat de Barcelona, Martí i Franquès 1-11. E-08028 Barcelona, Spain; E-Mails: marta.pujol@ub.edu (M.P.); jonathan.simo@ub.edu (J.S.); elia.sevilla@ub.edu (E.S.)

[2] Unitat de Difracció de Raigs-X, Centre Científic i Tecnològic de la Universitat de Barcelona, Solé i Sabarís 1-3, E-08028 Barcelona, Spain; E-Mail: mercefont@sct.ub.es

[3] Biomed Division, Leitat Tecnological Center, Parc Científic de Barcelona, Edifici Hèlix, C/Baldiri i Reixach, 15-21, E-08028 Barcelona, Spain; E-Mails: rmesseguer@leitat.org (R.M.); ccalvis@leitat.org (C.C.)

* Authors to whom correspondence should be addressed; E-Mails: conchi.lopez@qi.ub.es (C.L.); ramon.bosque@qi.ub.es (R.B.); Tel.: +34-93-403-91-34; Fax: +34-93-490-77-25.

External Editor: Axel Klein

Received: 31 July 2014; in revised form: 8 October 2014 / Accepted: 10 October 2014 / Published: 6 November 2014

Abstract: The study of the reactivity of the enantiopure ferrocenyl Schiff base (*S*$_C$)-[FcCH=N–CH(Me)(C$_6$H$_5$)] (**1**) (Fc = (η^5-C$_5$H$_5$)Fe(η^5-C$_5$H$_4$)) with *cis*-[PtCl$_2$(dmso)$_2$] under different experimental conditions is reported. Four different types of chiral Pt(II) have been isolated and characterized. One of them is the enantiomerically pure *trans*-(*S*$_C$)-[Pt{κ^1-*N*[FcCH=N–CH(Me)(C$_6$H$_5$)]}Cl$_2$(dmso)] (**2a**) in which the imine acts as a neutral *N*-donor ligand; while the other three are the cycloplatinated complexes: [Pt{κ^2-*C*,*N*[(C$_6$H$_4$)–N=CHFc]}Cl(dmso)] (**7a**) and the two diastereomers {*(S*$_p$,*S*$_C$*)* and *(R*$_p$,*S*$_C$*)*} of [Pt{κ^2-*C*,*N*[(η^5-C$_5$H$_3$)–CH=N–{CH(Me)(C$_6$H$_5$)}]Fe(η^5-C$_5$H$_5$)}Cl(dmso)] (**8a** and **9a**, respectively). Isomers **7a**-**9a**, differ in the nature of the metallated carbon atom [C^{Ph} (in **7a**) or C^{Fc} (in **8a** and **9a**)] or the planar chirality of the 1,2-disubstituted ferrocenyl unit (**8a** and **9a**). Reactions of **7a**–**9a** with PPh$_3$ gave [Pt{κ^2-*C*,*N*[(C$_6$H$_4$)–N=CHFc]}Cl(PPh$_3$)] (in **7b**) and the diastereomers *(S*$_p$,*S*$_C$*)* and *(R*$_p$,*S*$_C$*)* of [Pt{κ^2-*C*,*N*[(η^5-C$_5$H$_3$)–CH=N–{CH(Me)(C$_6$H$_5$)}]

Fe(η^5-C_5H_5)}Cl(PPh_3)] (**8b** and **9b**, respectively). Comparative studies of the electrochemical properties and cytotoxic activities on MCF7 and MDA-MB231 breast cancer cell lines of **2a** and cycloplatinated complexes **7b-9b** are also reported. Theoretical studies based on DFT calculations have also been carried out in order to rationalize the results obtained from the cycloplatination of **1**, the stability of the Pt(II) complexes and their electrochemical properties.

Keywords: platinacycles; chiral platinum(II) complexes; DFT calculations; biological activity; electrochemistry

1. Introduction

Cyclometallated platinum (II) complexes containing bidentate $(C,N)^-$ or terdentate $((C,N,E)^q$, $(N,C,E)^q$, (E = N, S or O and q = −1 or −2) or $(C,N,C')^{2-}$) ligands are nowadays one of the most attractive type of organoplatinum compounds [1–10]. This is mainly due to their physical, chemical, photo-physical and electrochemical properties, or the reactivity of their ground and excited states that make them extremely useful in a wide range of fields [1–10]. It is well-known that platinacycles are valuable precursors in homogeneous catalysis, as building blocks in supra- and macromolecular chemistry as well as for the synthesis of organic compounds (including natural products) and other organometallic products (*i.e.*, cyclometallated Pt(IV) derivatives) [11–15]. Sensors, detectors, biomarkers, molecular machines (*i.e.*, switches), imaging probes and different sorts of OLEDs (including white and white polymer light-emitting diodes (WOLED and PGOLED), respectively) containing cycloplatinated cores have been described [16–25]. Furthermore, cyclometallated Pt(II) complexes with antitumoral activity have been known for a long time, but the idea of using this sort of products in drug discovery is becoming more and more popular [15,26–33]. For illustrative purposes recent examples of platinacycles with bidentate $(C^{Ph}, N)^-$ ligands showing greater cytotoxic activity than cisplatin are shown in Figure 1 [29,32,33].

Figure 1. A selection of cyclometallated Pt(II) complexes with a σ(Pt-C^{Ph}) bond and potent cytotoxic activity reported recently. For illustrative purposes IC_{50} values (in μM) for **A**–**C** in a specific cancer cell line are given: in HCT-116 colon cell line for **A** compounds: IC_{50} = 28 ± 2.4 μM (R^1 = H) and 18 ± 1.9 μM (R^1 = Cl); for type **B**, IC_{50} in the range 0.95 μM–7.7 μM (IC_{50} for cisplatin = 40 ± 4.4 μM). Compound **C** was tested in the A549 breast cancer cell line, IC_{50} = 4.60 μM (for cisplatin = 8.0 μM) [29–32].

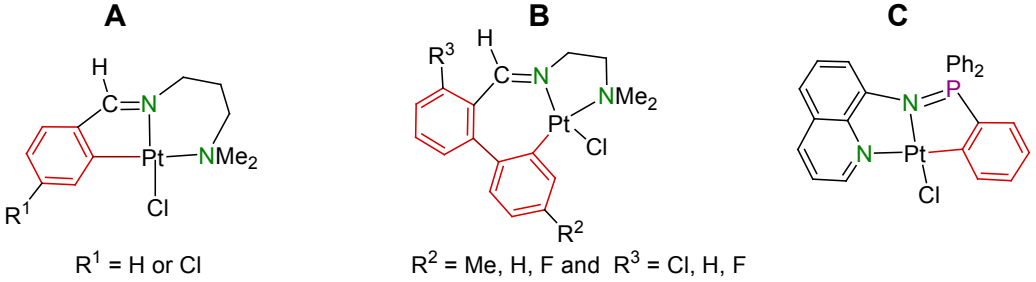

It is well-known that the properties of cycloplatinated compounds, their biological or catalytical activities and their applications are strongly dependent on a wide variety of factors, such as the nature of the donor atoms of the metallated ligand, its denticity, the size of the metallacycle, the electronic and steric effects induced by the presence of substituents and their location and even the nature of the ancillary ligands and their relative arrangement [1–10].

On the other hand, *N*-donor ferrocenyl ligands are valuable reagents to achieve heterodimetallic Pt (II) compounds [34–43]. These ligands may produce different types of products depending on the relative arrangement between the *N*-donor atom and the presence of: (a) one or more σ(C–H) bonds, with the proper orientation as to undergo metallation, and/or (b) additional heteroatoms with good donor abilities and their location [36,37,40,41]. Moreover, for monosubtituted ferrocene derivatives metallation of the C_5H_4 ring induces planar quirality [34,35,38]. Despite the variety of cyclometallated Pt(II) complexes derived from achiral *N*-donor ligands described so far, enantio- or diastereomerically pure platinacycles are scarce [39–47] and those containing a Pt–C^{Fc} bond are even less common [39–43]. However, the examples described so far are especially outstanding because of their singular properties, behaviors or activities [39–43]. A few representative examples (**A**–**D**) are shown in Figure 2. Compound **A** is an excellent catalyst on the asymmetric aza-Claisen rearrangement of Z configured trifuoroacetaamidates giving high enantioselectivities [39] and diastereomers **B** and **C** (Figure 2), form an acid-base dependent chiral molecular switch [40,41]. Platinacycles **D** and **E** are potent cytotoxic agents in lung (A549), breast (MDA-MB231) and colon (HCT-116) cell lines. Moreover, complex **E**: (a) is less toxic than cisplatin and active in other cancer cell lines (*i.e.*, NCI-H460); (b) induces nuclear translocation of endogenous FOXO3a and a FOXO3a reporter protein in A549 and U2OS cells, respectively; and (c) has a synergic effect with cisplatin [42,43].

Figure 2. Representative examples of diastereomerically pure cyclometallated Pt(II) complexes containing a σ(Pt–C^{Fc}) bond [39–43]. (For types **B** and **C**, *R* is Me or ^{i}Pr).

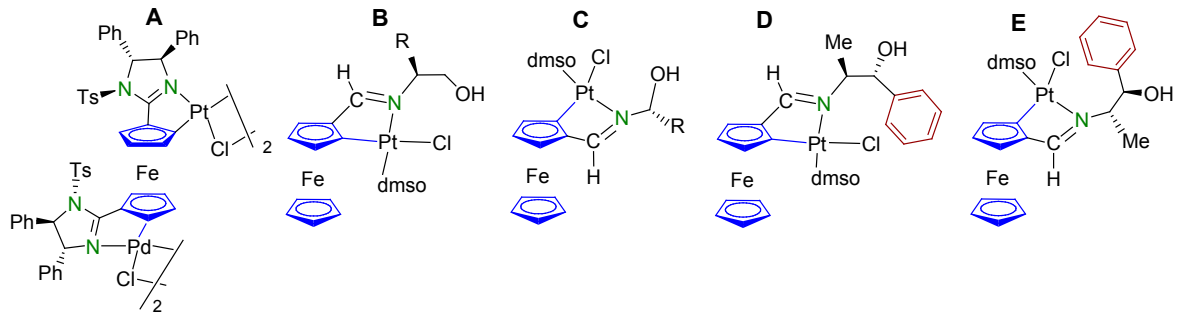

All these findings suggest that compounds containing simultaneously ferrocenyl units and cycloplatinated rings are promising candidates for the design of multifunctional products with both biological activity and interesting electrochemical properties (due to the presence of a redox active center). This is still an emerging topic and further work is needed to clarify some key points. Unfortunately, isomeric platinacycles differing exclusively in the nature of the metallated carbon have not been described so far, and thus the effect produced by the characteristics of the carbon atom bound to the Pt(II) (*i.e.*, C^{Fc} *versus* C^{Ph}) on their properties and activities still remains unknown.

Since during the preparation of **D** and **E** (Figure 2), no evidences of the formation of platinacycles arising from the metallation of the phenyl ring were detected [42], we decided to investigate whether

for (*S*C)-[FcC(H)=N–CH(Me)(C$_6$H$_5$)] (**1**) (Figure 3) [48], the relative orientation between the phenyl ring and the N atom and their proximity could also allow the isolation of platinacycles with a Pt–C^{Ph} bond.

Figure 3. Schiff base **1** selected for this study and schematic view of the different types of Pt(II) complexes (**2**–**11**) that may be formed. Compounds **2-11** differ in the conformation of the ligand (*anti*-(*E*) in **2**, **4**, **6**, **8**–**11** or *syn*-(*Z*) in **3**, **5** and **7**), the binding mode of the imine ((N) in **2**–**5**, (C,N)$^-$ in **6**–**9** or (C,N,C')$^{2-}$ in **10** and **11**), the type of metallated C atom (C^{Ph} in **6** and **7** or C^{Fc} in **8** and **9**), the number of Pt–C bonds contained (one in **6**–**9** or two in **10** and **11**) or the planar chirality of the Fc unit (S_p in **8** and **10** or R_p in **9** and **11**). (*X*, *L* = monoanionic and neutral ligand, respectively).

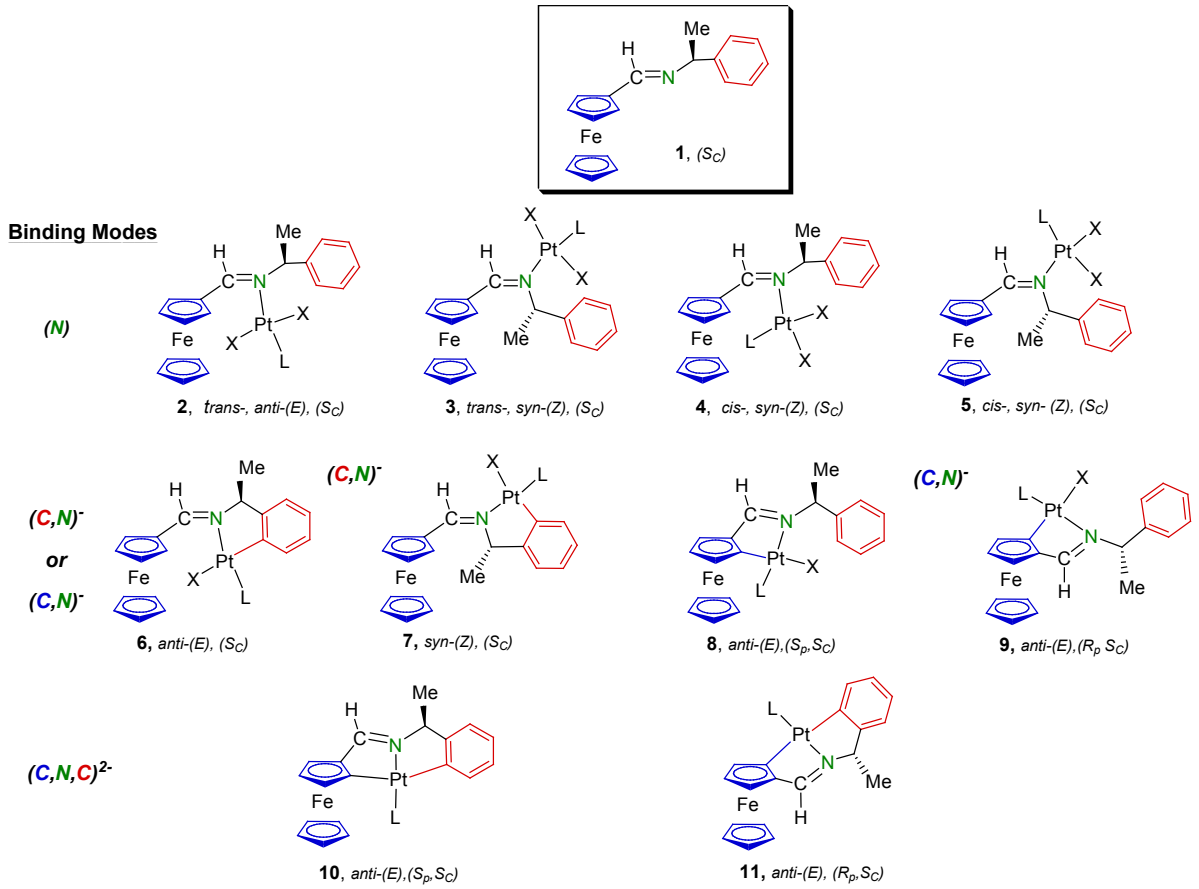

Ligand **1** may exhibit different binding modes and hapticities giving a wide variety of Pt(II) complexes (Figure 3). If **1** binds to the Pt(II) atom through the imine nitrogen exclusively, different isomeric forms of the optically active complexes: [Pt{κ^1-*N*[FcC(H)=N–CH(Me)(C$_6$H$_5$)]}*X*$_2$(*L*)] could be expected (**2**–**4** in Figure 3). They differ in the *anti*-(*E*) (in **2** and **3**) or the *syn*-(*Z*) (in **4** and **5**) form of the imine and a *trans*- (in **2** and **4**) or *cis*- (in **3** and **4**) disposition of the *X*$^-$ ligands. Moreover, **1** has several carbon atoms susceptible to undergo metallation. Four types of platinacycles (Figure 3, **6**–**9**) could arise from monometallation of **1**. In two of them (**6** and **7**) there is a σ(Pt–C^{Ph}) bond, and the imine adopts the *anti*-(*E*) (in **6**) or *syn*-(*Z*) (in **7**) forms; while the other two (**8** and **9**) are diastereomers (S_p,*S*C) and (R_p,*S*C) arising from platination of the C$_5$H$_3$ ring that induces planar chirality [34,35,38].

A few examples of cyclometallated Pt(II) compounds with (C,N,C)$^{2-}$ pincer ligands have been reported [49–52], and thus the activation of a σ(C^{Ph}–H] and a σ(C^{Fc}–H] bond to give compounds **10** or **11** (Figure 3) cannot be disregarded. Furthermore, and since several groups have achieved cylometallated

Pt(IV) complexes in the reaction of *cis*-[$PtCl_2(dmso)_2$] with *N*-donor ligands [23,53,54], the formation of the platinum(IV) derivatives cannot be ruled out either.

In this work, we report: (a) the synthesis of chiral Pt(II) complexes in which **1** adopts different binding modes {(N), (C^{Fc}, N)$^-$ or (C^{Ph}, N)$^-$}, (b) a comparative study of their electrochemical and cytotoxic activities in two breast cancer cell lines, and (c) a theoretical study based on DFT calculations to explain the selectivity of the metallation process and the properties of the new Pt(II) compounds.

2. Results and Discussion

2.1. Synthesis and Characterization of the Compounds

Treatment of equimolar amounts of (S_C)-[$FcC(H)=N–CH(Me)(C_6H_5)$] (**1**) and *cis*-[$PtCl_2(dmso)_2$] under reflux for 2 h, followed by work up of a SiO_2 column chromatography, gave traces of ferrocenecarboxaldehyde (FcCHO, 12 mg) and two new Pt(II) compounds in a molar ratio 1.00:0.13 (Scheme 1, step **A**).

Scheme 1. Synthesis of the new Pt(II) complexes: (i) *cis*-[$PtCl_2(dmso)_2$] in refluxing MeOH (2 h) followed by SiO_2 column chromatography; (ii) *cis*-[$PtCl_2(dmso)_2$] and NaOAc in a toluene:MeOH (4:1) mixture {molar ratios **1**:Pt(II):OAc^- = 1:1:2} under reflux (see text) followed by SiO_2 chromatography; (iii) PPh_3 in CH_2Cl_2 under reflux for 1 h; (iv) separation of the diastereomers by SiO_2 column chromatography.

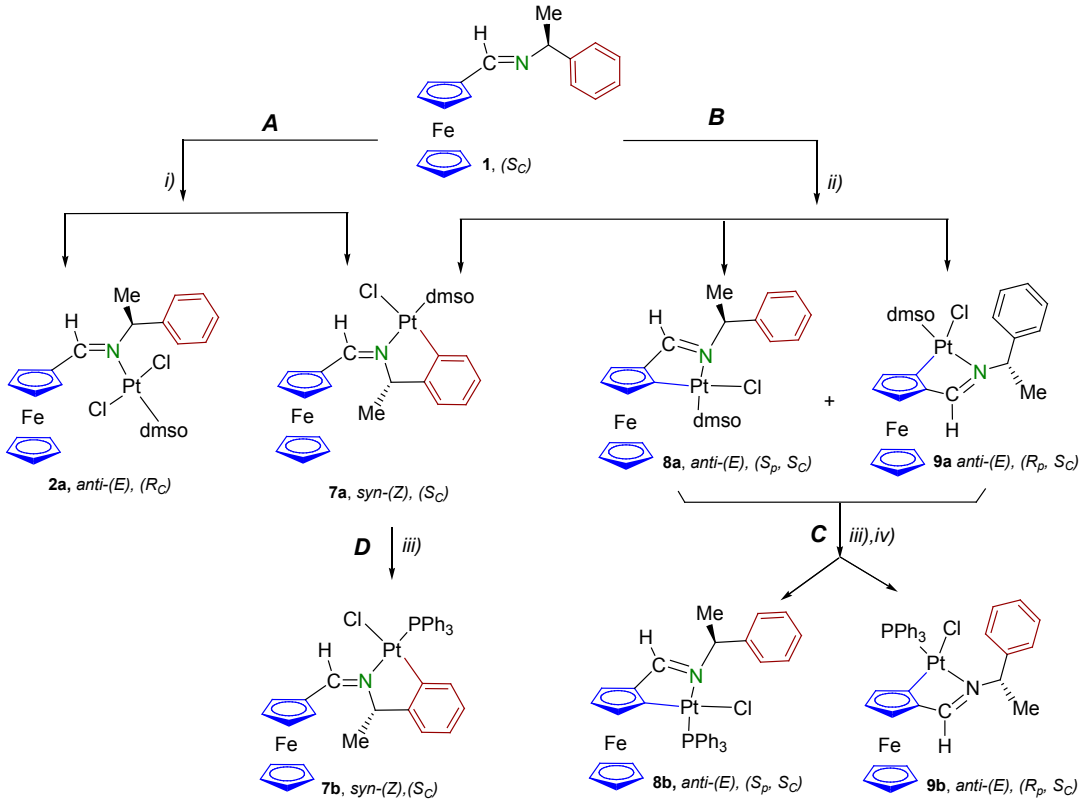

Elemental analyses and mass spectra of the major component (Supporting Information) were consistent with those expected for any of the four isomers of [Pt(**1**)Cl_2(dmso)] (Figure 3, types **2**–**5** with *X* = Cl and *L* = dmso (**2a**–**5a**)). In the ^{1}H-NMR spectrum the signals due to the protons of the

dmso ligand appeared as one singlet at δ = 3.40 ppm ($^3J_{H,Pt}$ = 19 Hz). This is characteristic of *trans*-[Pt{κ^1-*N*[FcC(R^1)=N–R^2]}Cl$_2$(dmso)] (*R*^{1} = H or Me) complexes [20,36,40–42]. Moreover, in its (^{1}H–^{1}H) NOESY spectrum, the signal of the imine proton showed cross peaks with those of the H^2 and H^5 protons of the Fc unit, and also with the resonances of the –CH(Me)-moiety. Thus indicating that imine **1** adopts the *anti*-(*E*) form. All these features suggested that in the major product the arrangement of the ligands corresponded to type **2** shown in Figure 1 (with *X* = Cl and *L* = dmso, herein after referred to as **2a**).

Its X-ray crystal structure (Figure 4) consists of discrete molecules of *trans*-[Pt{κ^1-*N*[(η^5-C$_5$H$_5$)Fe[(η^5-C$_5$H$_4$)–CH=N–CH(Me)(C$_6$H$_5$)]}Cl$_2$(dmso)] separated by van der Waals contacts. In each molecule, the Pt(II) is bound to the imine nitrogen, the sulphur of the dmso ligand and to the Cl(1) and Cl(2) atoms, in a *trans*- arrangement [bond angle Cl(1)–Pt–Cl(2) = 176.7(1)°], giving a slightly distorted square-planar environment around the Pt(II) atom. The Pt-ligands' bond lengths agree with those reported for *trans*-[Pt(imine)Cl$_2$(dmso)] compounds [20,41,55,56].

Figure 4. Molecular structure and atom labelling scheme for *trans*-(*S*$_c$)-[Pt{(η^5-C$_5$H$_5$)Fe[(η^5-C$_5$H$_4$)–CH=N–CH(Me)(C$_6$H$_5$)]Fe(η^5-C$_5$H$_5$)}Cl$_2$(dmso)] (**2**). Selected bond lengths (in Å) and angles (in deg.): Pt–N, 2.017(5); Pt–S, 2.206(2); Pt–Cl(1), 2.266(3); Pt–Cl(2), 2.280(3); C(10)–C(11), 1.424(12); C(11)–N, 1.261(9); N–C(12), 1.481(11); C(12)–C(13), 1.516(15); C(12)–C(14), 1.532(13); C(14)–C(15), 1.321(15); C(15)–C(16), 1.409(17); C(16)–C(17), 1.32(2); C(17)–C(18), 1.45(2); C(18)–C(19), 1.377(19); C(19)–C(14), 1.404(13); S–O, 1.444(8); S–Pt–Cl(1), 92.82(10); S–Pt–Cl(2) ,90.0(1);N–Pt–Cl(1), 88.4(2); N–Pt–Cl(2), 88.6(2); C(6)–C(10)–C(11), 118.9(8); C(9)–C(10)–C(11), 132.1(7); C(10)–C(11)–N, 128.6(7); C(11)–N–C(12), 116.0(6); N–C(12)–C(13), 111.2(8); N–C(12)–C(14), 112.9(8); O–S–C(20), 107.3(7); O–S–C(21), 107.6(6) and C(20)–S–C(21), 102.7(8).

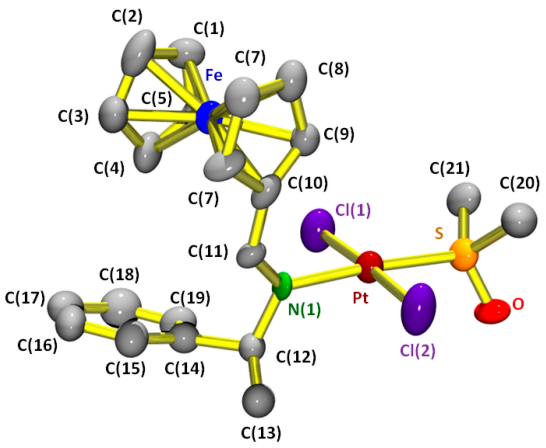

The imine is in *anti*-(*E*) form [torsion angle C(10)–C(11)–N(1)–C(12) = 175.9°] in good agreement with the conclusions reached by NMR and the C(10)–N(1) bond length (1.261(9) Å) is similar to that reported for [Pd(**1**)(η^3-C$_3$H$_5$)Cl] [1.255(6) Å] [48]. Bond lengths and angles of the Fc moiety are similar to those reported for most monosustituted ferrocenes [55,57]; the two pentagonal rings are planar, nearly parallel (tilt angle = 2.9°) and they deviate by 10.6(5)° from the ideal eclipsed conformation. The Fe(II)···Pt(II) distance (4.748 Å) precludes the existence of any direct interaction.

In the crystals, molecules are connected by weak Cl···H intermolecular interactions between: (a) the Cl(1) and the H(3) of a close molecule at (1 − *x*, −1/2 − *y*, 1/2 − *z*) (distance Cl(1)···H(3) = 2.894(8) Å) and (b) the Cl(2) and the H(15) atoms of another unit located at (1/2 + *x*, 5/2 − *y*, −*z*), (Cl(2)···H(15) = 2.690(7) Å) forming chains. These chains are connected through additional C(17)−H(17)···O and C(21)−H(21)··· π (C(6)−C(10) ring) interactions.

Elemental analyses and mass spectra of the minor component (**I**) were consistent with those expected for any of the platinacycles with $(C,N)^-$ bidentate ligands (types **6**–**9**, in Figure 2 with *X* = Cl and *L* = dmso (**6a**–**9a**)}. In the ^{1}H-NMR spectrum: (a) the resonances of the protons of the dmso appeared as a singlet, this is consistent with *trans*-arrangement of the dmso and imine nitrogen; and (b) the signal of the imine proton (at δ = 8.91 ppm, ($^4J_{H,Pt}$ = 51 Hz)) was low-field shifted in relation to the free ligand (δ = 8.20 ppm) [48]. This suggested, according to the bibliography [20,36,37,40–42], that **1** adopted the *syn*-(*Z*) form. Besides that, only four cross peaks were detected in the aromatic region of the {^{1}H–^{13}C}-HSQC spectra, indicating the existence of a Pt−C^{Ph} bond in the complex. The ^{195}Pt chemical shift was similar to those of complexes with "Pt(C^{Ph} ,N)ClS(dmso)" cores. All these findings indicate that **I** was [Pt{κ^2-*C*,*N*-[(C_6H_4)−CH(Me)−N=C(H)Fc]}Cl(dmso)] (Figure 3, type **7**, with *X* = Cl and *L* = dmso (**7a**)). Moreover, since it has been demonstrated that cyclometallation of enantio- or diastereomerically pure *N*-donor ferrocenyl ligands does not modify the chirality of the stereogenic center [40–42,58–60], the absolute configuration of **7a** is S_C.

It should be noted that: (a) the molar ratio **2a**:**7a** did not vary significantly when the reaction period (*t*) increased from 2 h (1.00:0.13) to 2 days (1.00:0.15), and (b) no evidences of the presence of platinacycles with σ[Pt−C(ferrocenyl)] bonds were detected by ^{1}H-NMR of the crude of the reactions. In view of these and since the formation of platinacycles with bidentate (C^{Ph} or C^{Fc}, N)]$^-$ ligands commonly requires the presence of a base (*i.e.*, NaOAc or the ligand itself), [20,36,37,40–42], we also studied the reactivity of **1** toward Pt(II) in the presence of NaOAc.

Treatment of ligand **1** with *cis*-[$PtCl_2$(dmso)$_2$] and NaAcO (in a molar ratio **1**:Pt(II):OAc^- = (1:1:2)) in a mixture of toluene: MeOH (4:1) under reflux for 2 h (Scheme 1, step **B**) followed by the work-up of a chromatographic column, gave small amounts of FcCHO (18 mg), compounds **2a**, **7a** and traces (*ca.* 9 mg) of a purple solid (hereinafter referred to as **II**). Elemental analyses of **II** agreed with those expected for the platinacycles with **1** acting as a $(C,N)^-$ ligand. Its ^{1}H-NMR spectrum showed two sets of superimposed signals (of relative intensities 1.00:0.90) with the typical pattern of 1,2-disubstituted ferrocene derivatives. Thus, indicating the presence of two species with a Pt−C^{Fc} bond in solution. Since metallation of the C_5H_4 ring induces planar chirality [20,38,40–42,58–60], two diastereomers ((S_p, S_C) and (R_p,S_C)) could be expected in principle (Figure 3, types **8** and **9** with *X* = Cl and *L* = dmso (**8a** and **9a**, respectively)). Consequently **II** contains a mixture of both isomers. Longer reaction periods (up to 6 days) produced significant variations of the relative abundance of **2a**, **7a** and **II**, (from 1.00:0.21:0.09 (for *t* = 2 h) to 1.00:0.46:0.64 (for *t* = 2 days)); and after 6 days, the typical resonances of **2a** were not detected in the ^{1}H-NMR spectrum of the crude of the reaction and only FcCHO, **7a** and **II** were isolated after the work up of the column. These results suggested that the formation of isomers (**8a** and **9a**) was slow.

Since: (a) the crystal structure of **2a** revealed that the C−H bond of the ferrocenyl unit is quite close to the Pt(II) ion (distance Pt···H(9) = 2.866 Å); and (b) the relative proportion **2a**: **II** decreased with time; we tentatively assumed that probably **2a** was the precursor of the mixture **II**. In order to test this hypothesis, compound **2a** was treated with NaOAc (in a 1:2 molar ratio) in toluene:MeOH (4:1) under

reflux for 6 days and then filtered and concentrated to dryness. NMR studies revealed the presence of FcCHO and the two diastereomers of **II** in a relative ratio (1.00:0.86) which is close to that obtained when the reaction was performed using ligand **1**, *cis*-[$PtCl_2(dmso)_2$] and NaAcO (1.00:0.90).

All the results presented here reveal that despite it is well-known that ferrocene derivatives are more prone to undergo electrophilic attacks than their phenyl analogues [34,35,58,61], for **1**, that has different types of σ(C−H) bonds susceptible to metallate, the formation of the platinacycle **7a** with a σ[Pt−C(phenyl)] is achieved under milder experimental conditions than those required to isolate the **8a** and **9a** with a σ[Pt−C(ferrocenyl)] bond. Unfortunately, attempts to separate the two components of **II** by fractional crystallisation or SiO_2 column chromatography failed and only solids enriched in *ca.* 70%–80% could be isolated by successive chromatographic columns.

Since it is well-known that platinacycles with PPh_3 ligands are more cytotoxic than their dmso analogues, we decided to study the reactivity of the platinacycles with PPh_3. As expected, treatment of **II** with the equimolar amount of PPh_3 gave the diastereomers (R_p, S_C) and (S_p, S_C) of [Pt{{κ^2-*C*,*N*-[(η^5-C_5H_3)−CH=N−CH(Me)(C_6H_4)]Fe(η^5-C_5H_5)}Cl(PPh_3)] (**8b** and **9b**, respectively) that could be isolated after a careful work-up of a SiO_2 column (Scheme 1, step **C**). In order to compare the electrochemical properties and the cytotoxic activities of isomeric compounds differing only in the nature of the metallated carbon, we also transformed platinacycle **7a** in CH_2Cl_2 following identical procedure and we isolated the (S_C)-[Pt{κ^2-*C*,*N*-[(C_6H_4)−CH(Me)−N=C(H)Fc}Cl(PPh_3)] (**7b**) (Scheme 1, step **D**).

Characterization data of **7b**–**9b** (Supplementary Information) agreed with the proposed formulae. $^{31}P\{^1H\}$-NMR data for **7b** (δ = 19.1 ($^1J_{Pt-P}$ = 3801 Hz)), **8b** (δ = 15.9 ($^1J_{Pt-P}$= 4191 Hz)) and **9b** (δ = 15.7 ($^1J_{Pt-P}$ = 4202 Hz)) are similar to those reported for related platinacycles with "(C^{Ph} or C^{Fc}, N,P,Cl)" cores and a *trans*- arrangement of the PPh_3 ligand and the imine nitrogen in good agreement with the transphobia effect [61]. ^{195}Pt NMR spectra of compounds **7b**–**9b** showed a doublet due to coupling with the ^{31}P-nucleus since it is well-known that an upfield shift in ^{195}Pt NMR is related to a strong donor interaction [62,63], Thus, differences detected in the ^{195}Pt chemical shifts of **7b** and those of **8b** and **9b** can be taken as a measure of the different donor abilities of imine **1** adopting the (C^{Ph},N)$^-$ or the (C^{Fc},N)$^-$ binding mode.

At this point and due to the increasing interest in platinacycles with (C,N,C')$^{2-}$ pincer ligands we turned our attention to **8b** and **9b**. Molecular models revealed that in both isomers the C−H bond on the ortho site of the phenyl ring has the proper orientation as undergo metallation to give platinacycles with **1** acting as a (C^{Fc},N, C^{Ph})$^{2-}$ pincer ligand (Figure 2, types **10** and **11** with *X* = Cl and *L* = PPh_3 (**10b** and **11b**)) and having central and planar chirality. In view of this, we also studied the reactions of the **8b** (or **9b**) with equimolar amounts of a NaOAc under reflux for 2 days in the toluene: MeOH (4:1) mixtures. However, no significant change was observed and ^{1}H-NMR spectra of the raw materials did not reveal the presence of any new Pt(II) complex.

As mentioned above, isomeric cycloplatinated complexes differing exclusively in the nature of the metallated carbon or the planar chirality of the metallated ferrocenyl moiety are scarce and studies on chiral derivatives are even less common. In view of this and mainly due to the ongoing interest in: (a) the potential antitumoral activity of platinacycles [1,15,26–32,42–43] and (b) electrochemical properties of ferrocene derivatives and heteropolymetallic complexes with ferrocenyl ligands [34,35,40,41,59], we decided to use compounds **7b**–**9b** for preliminary studies on these fields.

2.2. Study of the Cytotoxic Activity

Two human breast cancer cell lines (MCF7 and MDA-MB231) were used to test the cytotoxic activity of complex **2a** and the platinacycles (**7b**–**9b**). For comparison purposes, cisplatin (as positive control) was also evaluated under the same experimental conditions. The IC_{50} values corresponding to the inhibition of cancer cell growth at 50% level are listed in Table 1.

Table 1. Summary of: (a) the cytotoxic activities (IC_{50} (μM)) of compound **2a** and the platinacycles **7b**–**9b** in the MCF7 and MDA-MB231 breast cancer cell lines [a]; and (b) their electrochemical properties (Electrochemical data (anodic (E_{pa}) and cathodic (E_{pc}) potentials, separation between peaks ($\Delta E = E_{pa} - E_{pc}$) and the ratio between the intensities of the anodic and cathodic peaks I_{pa}/I_{pc})) [b].

Compound	Binding mode of 1	Cytotoxic activity, IC_{50}		Electrochemical data			
		MCF7	MDA-MB231	E_{pa}	E_{pc}	ΔE	I_{pa}/I_{pc}
2a	N	>100	76 ± nd	0.076	0.006	0.070	1.08
7b	$(C^{Ph}, N)^-$	37 ± 4	29 ± 3	0.101	0.038	0.063	1.10
8b	$(C^{Fc}, N)^-$	11.4 ± 1.1	5.8 ± 0.8	−0.127	−0.197	0.070	0.98
9b	$(C^{Fc}, N)^-$	9.2 ± 0.9	4.3 ± 0.6	−0.157	−0.228	0.071	0.97

[a] IC_{50} values for cisplatin under identical experimental conditions = 19.4 ± 4.5 μM (in MCF7) and 6.3 ± 2.4 μM (in MDA-MB231); [b] Potentials (in V) are referred to the ferrocene/ferricinium couple.

The comparison of *in vitro* cytotoxic activities of **2a**, **7b**, **8b** and **9b** against the MCF7 and MDA-MB231 breast cancer cell lines (Table 1 and Figure 5**a**) shows that complex **2a**, where **1** acts as an N-donor group, did not show any significant effect on the MCF7 cell line and only a moderate activity in MDA-MB231 cell line and platinacycles **7b**–**9b** were more potent than **2a** in the two cell lines assayed. In fact, their potencies increase according to sequence (1).

$$\mathbf{2a} < \mathbf{7b} < \textit{cisplatin} < \mathbf{8b} \leq \mathbf{9b} \text{ (for MCF7 and MDA-MB231)} \quad (1)$$

Figure 5. (**a**) Comparative plot of the cytotoxic activities (IC_{50} values (μM)) of complexes **2a**, the platinacycles **7b**–**9b** and cisplatin in the MCF7 and MDA-MB231 breast cancer cell lines and (**b**) cyclic voltammograms (at a scan rate of 0.1 V × s^{-1}) of the new Pt(II) complexes containing the aldimine **1** acting as a neutral *N*-donor (in **2a**) or as a monoanionic ($(C^{Ph}, N)^-$ (in **7b**) or $(C^{Fc}, N)^-$ (in **8b** and **9b**)) ligand.

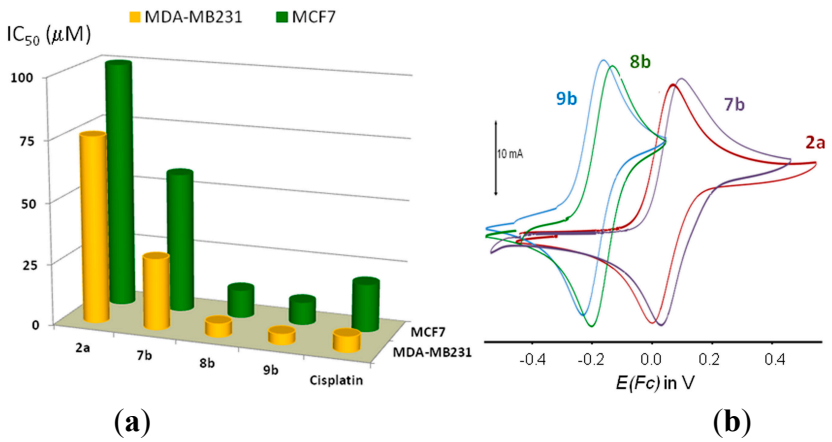

(**a**) (**b**)

Among the tested compounds, complex **2a** is a weaker cytotoxic agent than **7b**; while platinacycle **9b**, (and in a lesser extent, **8b**) are the most potent ones (IC_{50} in the ranges: 9–11 μM for MCF7 and 5.8–6.3 μM for the triple negative (ER, PR and no HER2 over expression) MDA-MB231 cell line). In particular, in particular the activity of **9b** is ca. 1.3 times (in MDA-MB231) or 2.1 times (in the MCF7) bigger than that of cisplatin. These findings indicate that platinacycles with Pt–C^{Fc} bond (**8b** and **9b**) are more active than **7b**, where the Pt(II) ion is bound to a C^{Ph} atom. The cytotoxic activity of the two diastereomers (**8b** and **9b**) is a bit different, if significant. This agrees with results obtained for compounds **D** and **E** (Figure 2) and suggest that the planar quirality of the metallated ring is not as important as the type of metallated carbon. Some authors have also found that for substituted ferrocene derivatives with stereogenic carbon atoms and their transition metal complexes, the absolute configuration does not affect significantly their cytotoxic activity [64–66].

Taking into account these results, trend (1) can be re-written as

$$(N) < (C^{Ph}, N)^{-} < (C^{Fc}, N)^{-} \quad (2)$$

that is a relationship between binding mode of **1** to the Pt(II) and the cytotoxic activity of the complexes.

2.3. Electrochemical Properties

In a first attempt to elucidate the effects produced by the mode of binding of the Schiff base to the Pt(II) atoms, and the nature of the metallated carbon atom on the electronic environment of the iron (II), we also studied the electrochemical properties of **2a**,**7b**, **8b** and **9b**. It should be noted that ^{1}H-NMR spectra of these products in CD_3CN revealed they were stable in this solvent. The electrochemical studies were carried out by cyclic voltammetry of freshly prepared solutions (10^{-3} M) in acetonitrile using $(Bu_4N)[PF_6]$ as supporting electrolyte. All these experiments were carried out at different scan rates υ (υ = from 0.05 to 1.0 V × s^{-1}). A summary of the electrochemical data for all the compounds under study is presented in Table 1.

The cyclic voltammograms (CVs) (Figure 5**b**) exhibited one anodic peak with a directly associated reduction in the reverse scan, intensities ratio I_{pa}/I_{pc} was close to 1.0 and the relationship between the I_{pa} and $\upsilon^{1/2}$ was lineal. These findings are consistent with those expected for a simple reversible one-electron process [67]. The main difference between the CVs of **2a**,**7b**,**8b** and **9b** is the position of the waves, that shift to the anodic region as follows:

$$\mathbf{9b} < \mathbf{8b} < < \mathbf{2a} < \mathbf{7b} \quad (3)$$

For the platinacycles **7b**–**9b** the trend is similar to that obtained for cyclopalladated compounds arising from the metallation of the Ph ring or the Fc unit of $(1S_C,2R_C)$-[(η^5-C_5H_5)Fe{(η^5-C_5H_4)−CH=N −CH(Me)-CH(OH)(C_6H_5)}] [59]. For the diastereomers **8b** and **9b**, the differences are small and fall in the ranges reported for the pairs of isomers (S_p,S_C) and (R_p,S_C) of [Pt{κ^2-*C*,*N*[(η^5-C_5H_3)−CH=N −CH(*R*)−CH_2(OH)]Fe(η^5-C_5H_5)}Cl(PPh_3)] (*R* = Me or ^{i}Pr) or (S_p,$1S_C$,$2R_C$) and (R_p,$1S_C$,$2R_C$) of [Pt{κ^2-*C*,*N*[(η^5-C_5H_3)−CH=N−CH(Me)−CH(OH)(C_6H_5)]Fe(η^5-C_5H_5)}Cl(PPh_3)] [40,41,59].

It is well-known that the proclivity of ferrocene derivatives to oxidize is strongly dependent on the nature of the substituents [41,59,61,67,68]. In general, the presence of electron withdrawing groups produces an increase of the E_{pa} value; while donor groups have the opposite effect. On these basis,

sequence (4) provides conclusive evidences of the influence of the binding mode of the ligand **1** to the Pt(II) on their the electrochemical properties of the complexes.

Compounds **8b** and **9b** with the $(C^{Fc},N)^-$ ligand are more prone to oxidize than **2a** where **1** binds to the Pt(II) through the N atom exclusively; while platinacycle **7b** is even more resistant to oxidation. Thus indicating that in **7b** the metallacycle has greater electron pulling effect on the ferrocenyl array than in **8b**, **9b**. Comparison of electrochemical data of platinacycles **7b**–**9b** and their biological activity, reveals that **7b** is simultaneously less prone to oxidize and a weaker cytotoxic agent than **8b** and **9b**. This relation shift has also been found for other ferrocene-containing compounds [69,70].

2.4. Theoretical Studies

In a first attempt to rationalise the experimental results and in particular, to explain: (a) why for **1** the cycloplatination of the phenyl ring occurs; and (b) the electrochemical properties of the Pt(II) complexes, we decided to undertake DFT calculations of the imine **1** [in the *anti-(E)* and *syn-(Z)* forms, herein after referred to as $\mathbf{1}^{\boldsymbol{E}}$ and $\mathbf{1}^{\boldsymbol{Z}}$, respectively], the isomers of [Pt{FcC(H)=CH(Me)(C_6H_5)}Cl_2(dmso)] (**2a** and **3a**) and platinacycles **6**–**9** of Figure 2 (*X* = Cl and *L* = dmso (**6a**–**9a**)).

All the calculations were carried out using the B3LYP hybrid functional [70,71] and the LANL2DZ basis set [72,73] implemented in the Gaussian03 program [74]. The geometries of compounds and were optimized without imposing any restriction. The bond lengths and angles of the optimized geometry of **2a** were consistent with those obtained from the X-ray studies (the differences did not clearly exceed 3σ).

For each one of the molecules under study in their optimized geometries the total energy (E_T) was calculated. The results obtained showed that the free ligand in the *syn*-(*Z*) conformation ($\mathbf{1}^{\boldsymbol{Z}}$) is 5.29 kcal/mol higher in energy than the *anti*-(*E*) isomer ($\mathbf{1}^{\boldsymbol{E}}$). Thus, suggesting that the energy required for the process $\mathbf{1}^{\boldsymbol{E}} \rightarrow \mathbf{1}^{\boldsymbol{Z}}$ (Scheme 2, step **A**) is expected to be small, but slightly greater than for the *anti-(E)→syn-(Z)* isomerization of the ligand in *trans*-[Pt{FcC(H)=CH(Me)−(C_6H_5)}Cl_2(dmso)] (**2a**) (Scheme 2, **B**).

Complex **2a** has several sites susceptible to metallate which would produce either **6a** (Scheme 2, step **C**) or the isomers **8a** and **9a** (Scheme 2, steps **D** and **E**); but for **3a** only the metallation of the phenyl ring, to give **7a**, is possible (Scheme 2, step **F**). In steps **C**–**F** the formation of the platinacycles requires the release of one of the Cl^- ligands and the activation of the corresponding σ(C−H) bond. On the other hand, the experimental work shows that despite the Fc unit is more prone to undergo electrophillic attacks than the phenyl ring [22], the formation of **7a** is achieved under milder experimental conditions than for **8a** and **9a**.

As a first approach to rationalize experimental results, first we determined the energy for the optimized geometries of **6a**–**9a**. The minimum value was obtained for **9a**; for **8a**, it was only 0.71 kcal/mol higher; but for **7a** and **6a** the calculated energies exceed, (by 4.05 and 16.42 kcal/mol, respectively), that obtained for **9a**.

We also calculated the energy variations for reactions **C**–**F**, where complex **2a** is transformed into the platinacycles **6a**, **8a** and **9a**; or **3a** into **7a**. These processes involve the activation of the C–H bonds and the formation of the monocycloplatinated products. Data presented in Scheme 2, indicate that from an energetic point of view: (a) for **2a**, metallation of the ferrrocenyl moiety to give **8a** and **9a** is

preferred over platination of the phenyl ring; and (b) the reaction **3a** → **7a**, requires a smaller energy income than steps **C**, **D** and **E**.

Scheme 2. Summary of the different processes studied by DFT calculations that involve: (a) the *anti*-(*E*) → *syn*-(*Z*) isomerization of the free ligand (**1**) or of compound **2a** (steps **A** and **B**, respectively); (b) the transformation of complex **2a** into platinacycles **6a**, **8a** and **9a** by activation of the σ(C^{Ph}–H) (step **C**) or the σ(C^{Ph}–H) bonds (steps **D** and **E**); (c) the conversion of complex **3a** into the platinacycle **7a** (step **F**) and d) the platination of the phenyl ring of **8a** or **9a** (steps **G** and H, respectively) to give the biscycloplatinated derivatives **10a** and **11a**. (The values below or next to the arrows are the variations of energies (in kcal/mol) for the corresponding step).

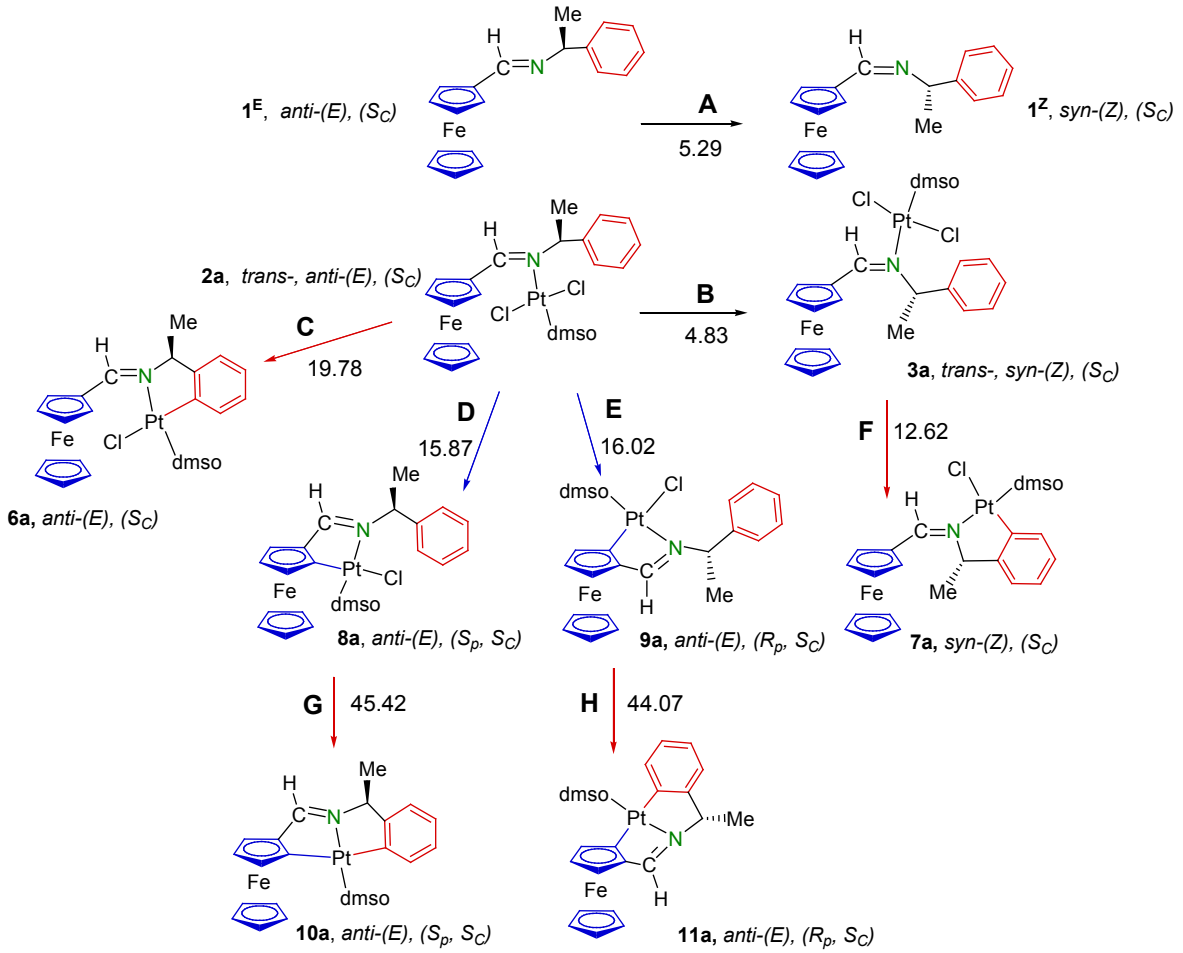

Using the E_T values for isomers **6a**–**9a** and T = 298 K, we also calculated the Boltzmann's distribution to estimate the relative proportion of the four isomers: 51.3 (for **8a**), 38.6 (for **9a**), 10.0 (for **7a**) and 0.1% (for **6a**). Except for **6a**, that was neither isolated nor detected in any of the reactions studied, the relative amounts of the isomers **7a**–**9a** formed when the reaction was performed using *cis*-[$PtCl_2(dmso)_2$], the ligand **1** and NaOAc (in a 1:1:2 molar ratio) follow the trend **7a** << **9a** < **8a** that is in good agreement with the results reached from the Boltzman's analyses.

Experimental work revealed that **2a** could be converted into **8a** and **9a**, but this process required the presence of a two fold excess of NaOAc and long refluxing periods (6 days). However, attempts to

achieve platinacycles with **1** acting as $(C^{Fc},N,C^{Ph})^{2-}$ from **8a** or **9a** failed. ΔE_T calculated for steps **G** and **H** of Scheme 2 is high (more than 2.7 times the ΔE_T of **D** or of **E**). This may explain why no evidences of the formation of compounds **10a** or **11a** were detected in any of the reactions investigated.

On the other hand, experimental results indicate the nature of the C atom bound to the Pt(II) in platinacycles **7b**–**9b** produces great changes in their electrochemical properties. Since the oxidation requires the removal of the electron from the highest occupied molecular orbital (HOMO), molecular orbital calculations were also performed for platinacycles **7a**–**9a**, for comparison purposes we also included complex **6a** in these calculations.

For **6a** and **7a**, the HOMO (Figure 6), is mainly formed by the contribution of a 5d orbital of the Pt(II), a 3p orbital of the chloride, and a π orbital of the metallated phenyl ring. The HOMOs of **8a** and **9a** are markedly different since they are mainly centered on the Fe(II) and the Pt(II) atoms. These findings confirm that for **6a**–**9a** the HOMO is not only iron based. For **6a**–**9a** LUMO orbitals (Figure 6) have a similar shape that results from the contribution of a π* orbital of the >C=N− group and to a lesser extent an atomic orbital of the Fe(II).

Figure 6. Highest occupied molecular orbital (HOMO) and LUMO orbitals for the cycloplatinated compounds **6a**–**9a**.

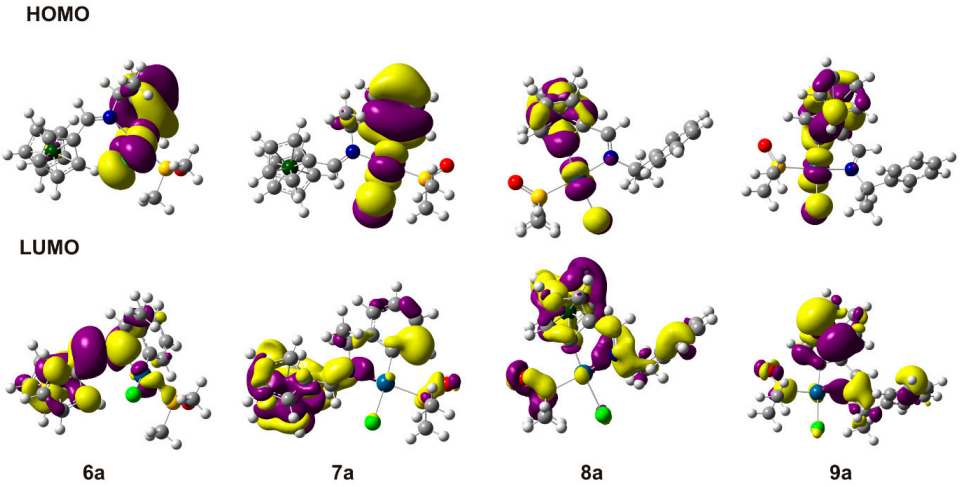

In order to explain the different proclivity of compounds **7b**–**9b** to undergo oxidation, we determined the energy of the HOMO (E_{HOMO}). As shown in Table 2 E_{HOMO} increases according to the sequence **6a** ≈ **7a** << **8a** ≤ **9a**, indicating that platinacycles **6a** and **7a**, with the $(C^{Ph}, N)^-$ ligand, are less prone to oxidize than their analogues formed by metallation of the Fc unit. This trend agrees with the results obtained from CV that revealed that **7b** less more prone to oxidize than **8b** or **9b**.

Table 2. Calculated energies (in hartrees) of the HOMO and LUMO (E_{HOMO} and E_{LUMO}, respectively) and energy gap (E_{LUMO}–E_{HOMO}) for the isomers **6a**–**9a** (shown in Scheme 2).

Compound	Binding Mode of 1	E_{HOMO}	E_{LUMO}	E_{LUMO}–E_{HOMO}
6a	$(C^{Ph}, N)^-$	−0.204	−0.058	0.146
7a	$(C^{Ph}, N)^-$	−0.204	−0.062	0.142
8a	$(C^{Fc}, N)^-$	−0.198	−0.054	0.144
9a	$(C^{Fc}, N)^-$	−0.193	−0.057	0.136

3. Experimental Section

3.1. Preparation of the Compounds

3.1.1. *trans*-(S_C)-[Pt{κ^1-*N*[FcC(H)=N−CH(Me)(C_6H_5)]}Cl_2(dmso)] (**2a**)

A suspension containing 250 mg (5.92×10^{-4} mol) of *cis*-[$PtCl_2$(dmso)$_2$] and 40 mL of MeOH (HPLC-grade) was refluxed until complete dissolution of the Pt(II) complex. Then, the hot solution was filtered out and filtrate was treated with 188 mg (5.92×10^{-4} mol) of ligand **1**. The reaction mixture was protected from the light with aluminium foil and refluxed for 2 h. After this period the solution was concentrated to dryness on a rotary evaporator, Afterwards the residue was dissolved in the minimum amont of CH_2Cl_2 and passed through a SiO_2-column chromatography (13.5 cm × 2.3 cm) using CH_2Cl_2 as eluant. The first band collected gave, after concentration to dryness small amounts of FcCHO (18 mg). Once this band was collected the subsequent elution with CH_2Cl_2 produced the release of an adidional and wide band, that contained complex **2a**. This band was collected and concentrated to *ca.* 5 mL. Slow evaporation of the solvent at 282 K produced the formation of small crystals of **2a** that were collected and air-dried. (yield: 275 mg, 70.2%).

3.1.2. *(S_C)*-[Pt{κ^2-*C*,*N*[(C_6H_4)(Me)CHN=C(H)Fc]}Cl(dmso)] (**7a**)

This compound was obtained as a minor side-product during the preparation of **2a**. and it was isolated from the column described in the preceding paragraph as follows. After the elution of the band containing **2a**, the column was eluted with a CH_2Cl_2: MeOH (100:0.5) mixture. This produced the release of a tiny and narrow band that was collected and concentrated to dryness on a rotary evaporator. The solid formed was air-dried and then dried in vacuum for 2 days (yield: 34 mg, 9.3%).

3.1.3. Synthesis of **II** {a Mixture of the (S_p, S_C) and (R_p, S_C) Diastereomers [Pt{κ^2-*C*,*N* [(η^5-C_5H_3)−CH=N−{CH(Me)(C_6H_5)}]Fe(η^5-C_5H_5)}Cl(dmso)] (**8a** and **9a**, respectively)

This mixture was obtained by using two alternative procedures (a and b) using either **1** and *cis*-[$PtCl_2$(dmso)$_2$] as starting materials (method a) or complex **2a** (method b).

Method a. Cis-[$PtCl_2$(dmso)$_2$] (250 mg, 5.92×10^{-4} mol) and imine **1** (188 mg, 5.92×10^{-4} mol) were treated with 40 mL of toluene. Afterwards, a solution formed by NaOAc (98 mg, 1.19×10^{-3} mol) and 10 mL of MeOH was added. The reaction mixture weas protected from the light with aluminum foil and refluxed for 6 days. After this period, the hot solution was filtered out and the filtrate was concentrated to dryness on a rotary evaporator. The residue was kept in a SiO_2 dissicator overnight. Then it was dissolved in the minimum amount of CH_2Cl_2 (*ca.* 10 mL) and passed through a SiO_2-column chromatography (13.5 cm × 2.3 cm) using CH_2Cl_2 as eluant. Concentration to dryness of the yellowish band eluted gave small amounts of FcCHO (22 mg). Then elution with a CH_2Cl_2: MeOH (100:0.5) mixture, produced two bands of which the first eluted one gave after evaporation of the solvent complex **7a** (42 mg). The second band that was purple and remained on the top of the column was later on collected increasing the polarity of the eluant to 100:1. The solid **II**, containing the two diastereomers (**8a** and **9a**, in a molar ratio 1.00:0.89), was isolated after concentration and the subsequent drying in vacuum for 2 days (140 mg).

Method b. Compound **2a** (120 mg, 1.8×10^{-4} mol) was dissolved in 20 mL of toluene, then a solution formed by 30 mg of NaOAc (3.6×10^{-4} mol) and 5 mL of MeOH was added. Then the flask containing the reaction mixture was protected from the light with aluminum foil and refluxed for 6 days. After this period, the nearly black solution was filtered through a Celite pad and the filtrate was concentrated to dryness on a rotary evaporator. The purple solid formed, that contained **8a** and **9a** (1.00:0.86), was washed with (3 × 5 mL portions) of n-hexane, air-dried and then dried in vacuum for 2 days (75 mg, 66%).

3.1.4. (S_C)-[Pt{κ^2-*C*,*N*[(C_6H_4)CH(Me)−N=C(H)Fc]}Cl(PPh_3)] (**7b**)

Complex **7a** (21 mg, 3.4×10^{-5} mol) was dissolved in 15 mL of CH_2Cl_2, then, PPh_3 (9 mg, 3.4×10^{-4} mol) was added. The reaction mixture was protected from the light with aluminum foil and refluxed for 1 h. After this period, the undisolved materials were removed by filtration and the pale orange filtrate was concentrated on a rotary evaporator to *ca.* 5 mL. The container was kept overnight on a refrigerator. After this period the solution was passed through a fast and short SiO_2 column (1.0 cm × 0.5 cm) using CH_2Cl_2 as eluant. The orange band released was collected and concentrated to dryness on a rotary evaporator. The solid formed was collected, air-dried and afterwards dried in vacuum for 2 days (yield: 27 mg, 69%).

3.1.5. Preparation of the Mixture of the Diastereomers of [Pt{κ^2-*C*,*N*[(η^5C_5H_3)−CH=N−CH(Me)(C_6H_5)]Fe(η^5-C_5H_5)}Cl(PPh_3)] (**8b** and **9b**)

To a solution containing 66 mg (1.02×10^{-4} mol) of the mixture of two diastereomers of [Pt{κ^2-*C*,*N*[(η^5-C_5H_3)−CH=N−CH(Me)(C_6H_5)]Fe(η^5-C_5H_5)}Cl(dmso)] (**8a** and **9a**) and 50 mL of CH_2Cl_2, PPh_3 (27 mg, 1.02×10^{-4} mol) was added. The reaction mixture was refluxed for 1 h and then filtered out. The filtrate was concentrated to *ca.* 5 mL and passed through a short SiO_2-column chromatography. The use of a CH_2Cl_2:MeOH (100: 0.2) mixture as eluant produced the release of a deep-orange band which was collected and concentrated to dryness on a rotary evaporator. Finally, the solid was dried in vacuum for 3 days and the two diastereomers in a *ca* 1.0:0.9 molar ratio (58 mg, 70%).

3.1.6. Separation of the Diastereomers of [Pt{κ^2-*C*,*N*[(η^5-C_5H_3)−CH=N−CH(Me)(C_6H_4)]Fe(η^5-C_5H_5)}Cl(PPh_3)] (**8b** and **9b**)

A 50 mg amount of the mixture of diastereomers (**8b** and **9b**) was dissolved in the minimum amount of CH_2Cl_2 and passed through a SiO_2 column (2.5 cm × 3.0 cm) using a CH_2Cl_2:MeOH (100:0.01) mixture as eluant. The purple band released was collected in *ca.* 20 mL portions up to a total volume of 180 mL and then concentrated to dryness on a rotary evaporator giving **9b** (23 mg). The solution obtained with the subsequent elution with 160 mL, lead after concentration, a mixture of the two isomers; while the final nine fractions collected produced isomer **8b** (19 mg).

4. Conclusions

The results presented in this work reveal that the enantiopure imine **1** is a valuable ligand to achieve different types of chiral heterodimetallic complexes containing Pt(II) and Fe(II). Among the organic compounds that exhibit a similar rich and versatile chemistry in the presence of Pt(II) atoms, ligand **1** is, to the best of our knowledge, the first that can: (a) generate a variety of chiral complexes with ferrocenyl units and (b) adopt three different binding modes ((N) (in **2a**), $(C^{Ph},N)^-$ (in **7a** and **7b**) or $(C^{Ph},N)^-$ (in **8a**, **8b**, **9a** and **9b**)), and thus leading to isomeric forms of cyclometallated Pt(II) complexes differing in Pt–C bond (C^{Ph} (in **7a** or **7b**) or C^{Fc} (in **8a**, **8b**, **9a** and **9b**)) or the planar chirality {S_p (in **8a** and **8b**) or R_p (in **9a** and **9b**)}. It has been reported that cyclopalladation of (*1S*$_C$, *2R*$_C$) [(η^5-C_5H_5)Fe{(η^5-C_5H_4)−CH=N−CH(R)−CH(OH)(C_6H_5)}] (*R* = Me or ^{i}Pr) gives palladacycles in which this imine acts as a $(C^{Fc},N)^-$ or $(C^{Ph},N)^-$ ligand [59], but for Pt(II) only the diastereomers (*S*$_p$,*1S*$_C$,*2R*$_C$) and (*R*$_p$,*1S*$_C$,*2R*$_C$) of [Pt{κ^2-*C*,*N*[(η^5-C_5H_3)−CH=N−CH(Me)−CH(OH)(C_6H_5)]Fe(η^5-C_5H_5)}Cl(dmso)] (**D** and **E** in Figure 2) were isolated. Thus, indicating that the intercalation of the "(*R*$_C$) –CH(OH)–" unit between the stereogenic carbon of **1** and phenyl ring is important as to hinder the formation of platinacycles with a Pt−C^{Ph} bond and a [6.6] bicyclic system (the six-membered metallacycle fused with the Ph ring).

Moreover, we have also demonstrated that an accurate control of the experimental conditions permits to control the preferential formation of a specific type of product as well as the nature of the C−H bond involved in the cycloplatination process. Although the selectivity of the cyclometallation process is low, it provides a simple method for achieving enantio- or diastereomerically pure organometallic Pt(II) complexes with one stereogenic carbon center and with (in **8a**, **8b**, **9a** and **9b**) or without (in **2a**, **7a** and **7b**) planar chirality which are extremely scarce, but attracting more and more interest due to their potential utilities and applications.

The new Pt(II) complexes presented herein appear to be excellent candidates for use not only as precursors in asymmetric synthesis or catalysis, but also as electrochemical reagents or as cytotoxic agents. For instance, an accurate selection of the product allows the fine-tuning of the anodic and cathodic potentials in a wide range (*i.e.*, E_{pa}(minimum) = −0.157 V (for **9b**) and E_{pa}(maximum) = 0.101 V (for **7b**)). Thus, these compounds are also attractive in view of their potential utility as selective and specific electrochemical sensors or detectors.

Computational studies have also allowed us to explain the effects produced by the nature of the metallated carbon atom on the relative stability of platinacycles with "Pt(C,N)(*X*)(*L*) cores" (Figure 2 **6**–**9**), the regioselectivity of the process and also the shift of the waves detected in the cyclic voltammograms.

On the other hand, the biological studies reveal that platinacycle **7b** is a weaker cytotoxic agent than cisplatin, but **8b** and **9b** are even more potent agents. This indicates that the binding mode of **1** in the platinacycles ($(C^{Ph},N)^-$ or $(C^{Fc},N)^-$) is important as to modify their biological activity. Moreover, the IC_{50} values of **8b** and **9b** in the MDA-MBD231 breast cancer cell line fall in the range obtained for compounds **D** and **E** (Figure 2), which exhibit a synergic effect with cisplatin [43]. These findings open up new research paths mainly focused on the following areas: (a) the evaluation of the cytotoxic effect of **8b** and **9b** in other cancer cell lines including some cisplatin resistant ones, such as HCT-116 colon cancer cell line; (b) additional studies to bring information about their mechanism of action; (c)

the chemical modification of the complexes *i.e.* by replacement of one or the two ancillary ligands to get neutral of ionic derivatives, to be tested on these two breast cancer cell lines.

Acknowledgments

This work was supported by the Ministerio de Ciencia e Innovación (CTQ2009-11501) of Spain.

Author Contributions

Synthesis and characterization of the new compounds (Marta Pujol, Jonathan Simó and Eila Sevilla), biological studies (Ramon Messeguer and Carme Calvis), X-Ray studies (Mercè Font-Bardía), electrochemical studies (Ramón Bosque and Concepción López), computational studies (Ramón Bosque), and the design of the experiments as well as the preparation of the manuscript (Concepción López).

Appendix

Description of materials and experimental methods used to characterize the compounds and to study their properties together with their characterization data (elemental analyses, mass spectra, IR-spectrocospic data, and NMR data). The crystallographic file information (cif. file) of compound **2a** has been deposited at the *Cambridge Crystallographic Data Centre* (reference code: CCDC-1016768) and can be obtained free of charge [75].

A1. Materials and Methods

A1.1. General

Ligand **1** and *cis*-$[PtCl_2(dmso)_2]$ were prepared as described previously [48,76]. The success of the synthesis of the Pt(II) compounds is strongly dependent on the quality of the methanol used. Methanol HPLC-grade is strongly required, because the presence of small amounts of water produces a significant decrease of the yields and increases the amount of FcCHO isolated. The remaining solvents used in this work were dried and distilled before use [77].

Elemental analyses were carried out at the *Serveis Cientifico-Tècnics* (Univ. Barcelona) and *Servei de Recursos Cientifics i Tècnics* (Univ. Rovira i Virgili, Tarragona). Proton and the two-dimensional NMR experiments ((^{1}H-^{1}H)-(COSY) and (NOESY) and the (^{1}H-^{13}C)-(HSQC) and (HMBC)) were run at 500MHz with either a Varian 500 or a Bruker (Billerica, MA, USA) Avance 500DMX instruments using $CDCl_3$ (99.9%) and $SiMe_4$ as reference). In order to test the stability of the complexes used in the electrochemical studies (**2a**, **7b**, **8b** and **9b**), their ^{1}H-NMR spectra were also registered in CD_3CN (99.8%) at 298 K.

^{195}Pt{^{1}H}- (of **7a**,**b**–**9a**,**b**) and ^{31}P{^{1}H} (of **7b**–**9b**) NMR spectra were recorded with a Bruker-250DXR (Billerica, MA, USA) instrument using $CDCl_3$ (99.9%) as solvent. The references were $P(OMe)_3$ and $H_2[PtCl_6]$ [δ^{31}P{$P(OMe_3)$} = 140.17 ppm and δ^{195}Pt{$H_2[PtCl_6]$} = 0 ppm], respectively. In all cases the chemical shifts (δ) are given in ppm and the coupling constants (*J*) in Hz. The optical rotations of **2a**, **7b**–**9b** were determined in CH_2Cl_2 at 298 K using a Perkin Elmer 241 MC

polarimeter and the concentration is specified in the characterisation section of the corresponding compound. Mass spectra (FAB^+) were obtained with a VG-Quatro Fisions instrument using 3-nitrobenzylalcohol (NBA) as matrix.

Table A1. Crystal data and structure refinement for *trans*-(*Sc*)-[Pt{κ^1-,*N*[FcC(H)=N–CH(Me)–(C_6H_5)]}Cl_2(dmso)] (**2a**).

Structural Parameter	Compound 2a
Crystal dimmensions/mm × mm × mm	0.2 × 0.1 × 0.1
Empirical formula	$C_{21}H_{25}Cl_2FeNO_2Pt$
Formula weight	661.32
T/K	293(2)
λ/Å	0.71073
Crystal system	Orthorhombic
Space group	$P2_12_12_1$
a/Å	11.670(10)
b/Å	13.2570(10)
c/Å	14.8780(10)
α = β = γ/°	90.0
Volume/Å^3	2202.6(3)
Z	4
Calculated density/Mg × m^{-3}	1.994
μ/mm^{-1}	7.353
F(000)	1280
Θ range for data collection/°	2.06 to 31.72
Limiting indices	$0 \le h \le 16, -19 \le k \le 19, -21 \le l \le 21$
Reflections collected/unique	9069/6010 [R(int) = 0.0705]
Completeness to Θ = 28.34°	95.2%
Absorption correction	Empirical
Max. and min. Transmission	0.48 and 0.42
Refinement method	Full-matrix least-squares on F^2
Data/restraints/parameters	6010/0/254
Goodness-of-fit on F^2	1.196
Final R indices [$I > 2\sigma(I)$]	R_1 = 0.0418, wR_2 = 0.1301
R indices (all data)	R_1 = 0.514, wR_2 = 0.1414
Absolute struture parameter	0.00(2)
Largest diff. peak and hole/e Å^{-3}	1.522 and −1.764

A1.2. Crystallography

A prismatic crystal of trans-[Pt{κ^1-N[FcC(H)=N–CH(Me)(C_6H_5)]}Cl_2(dmso)] (**2a**) (Table A1) was selected and mounted on a MAR345 diffractometer with a image plate detector. Unit-cell parameters were determined from 15,901 reflections in the range 3° ≤ Θ ≤ 31° and refined by least-squares method. Intensities were collected with a graphite monochromatised Mo-K_α radiation. The number of reflections measured in the range was 14,219 of which 6,010 were non-equivalent by symmetry (R_{int}(on *I*) = 0.0031) and 5106 reflections were assumed as observed applying the condiction $I > 2\sigma(I)$. Lorentz-polarisation and absorption corrections were made. The structure was solved by Direct methods using SHELXS computer program [78] and refined by full-matrix least-squares equation

using The SHELX97 computer program [79] using 6010 reflections (very negative intensities were not assumed). The function minimised was $\Sigma\ w\ \left|\ |F_o|^2 - |F_c|^2\ \right|$ where $w = [\sigma^2(I) + (0.0654P)^2 + 4.8984P]^{-1}$ and $P = (|F_o|^2 + 2|F_c|^2)/3$, were taken from the literature [80]. The chirality of the structure was determined from the Flack coefficient [81] which is equal to 0.00(2) for the given results. All hydrogen atoms were computed and refined using a riding model, with an isotropic temperature factor equal to 1.2 times the equivalent temparature factor of the atom linked to it. The final *R* factors as well as other relevant parameters concerning the resolution and refinement of the crystal structure are presented in Table A1.

A1.3. Biological Studies

A1.3.1. Cell Culture

Breast cancer MCF7 and MDA-MB231 cells (from *European Collection of Cell Cultures, ECACC*) were grown as a monolayer culture in minimum essential medium (DMEM with L-glutamine, without glucose and without sodium pyruvate) in the presence of 10% heat-inactivated fetal calf serum, 10 mM of D-glucose and 0.1% streptomycin/penicillin in standard culture conditions.

A1.3.2. Cell Viability Assays

For these studies, compounds were dissolved in 100% DMSO at 50 mM as stock solution; then, serial dilutions have been done in DMSO (1:1) (in this way DMSO concentration in cell media was always the same); finally, 1:500 dilutions of the serial dilutions of compounds on cell media were done. The assay was performed as described by Givens *et al.* [82]. In brief, MDA-MB231 and MCF7 cells were plated at 5,000 cells/well or 10,000 cells/well respectively, in 100 μL media in tissue culture 96 well plates (Cultek, Boston, USA). After 24 h, media was replaced by 100 μL/well of serial dilution of drugs. Each point concentration was run in triplicate. Reagent blanks, containing media plus colorimetric reagent without cells were run on each plate. Blank values were subtracted from test values and were routinely 5%–10% of uninhibited control values. Plates were incubated for 72 h. Hexosamidase activity was measured according to the following protocol: the media containing the cells was removed and cells were washed once with PBS 60 μL of substrate solution (*p*-nitrophenol-*N*-acetyl-β-D-glucosamide 7.5 mM (Sigma, San Luis,MO, USA N-9376), sodium citrate 0.1 M, pH = 5.0, 0.25% Triton X-100 (Sigma-Aldrich Quimica, Tres Cantos, Madrid, Spain), was added to each well and incubated at 37 °C for 1–2 h; after this incubation time, a bright yellow color appeared; then, plates could be developed by adding 90 μL of developer solution (Glycine 50mM, pH = 10.4; EDTA 5 mM), and absorbance was recorded at 410 nm.

A1.4. Electrochemical Studies

Electrochemical data for compounds under study were obtained by cyclic voltammetry under nitrogen at 298 K using acetonitrile (HPLC-grade) as solvent, tetrabutylamonium hexafluorophosphate {(Bu_4N)[PF_6]} (0.1 M) as supporting electrolyte and a M263A potentiostat from EG&G instruments. The half-wave potentials were referred to an Ag-$AgNO_3$) 0.1 M in acetonitrile) electrode separated from the solution by a medium porosity fritted disk. A platinum wire auxiliary electrode was used in

conjunction with a platinum disk working Tacussel-Edi electrode (3.14 mm^2). Cyclic voltammograms of ferrocene were preformed before and after each sample to ensure the repeatability of the results, in particular to test the stability of the Ag-$AgNO_3$ electrode. Cyclic voltammograms of freshly prepared solutions (10^{-3} M) of the samples in acetonitrile were run and potentials measured were the referred to the ferrocene that was used as internal internal reference. In these experimental conditions the standard error of the measured potentials is ± 5 mV. In all the experiments, the cyclic voltammograms were run using scan-speeds (v) in the range: 0.05 V $s^{-1} \leq v \leq$ 1.0 V s^{-1}.

A1.5. Theoretical Studies

Calculations were carried out at the B3LYP computational level [70,71] with the *Gaussian98* package [74] using LANL2DZ basis set [72,73]. Geometry optimizations were performed without any geometry restriction.

A2. Summary of Characterization Data for Compounds under Study (Atom Numbering Schemes for Compounds 2a, 7a, Diastereomers 8a and 9a, 7b, 8b and 9b Are Presented in Figures A1–A6, Respectively)

*A2.1. trans-(S$_C$)-[Pt{κ^1-N[FcC(H)=N–CH(Me)(C$_6$H$_5$)]}Cl$_2$(dmso)] (**2a**)*

Anal. (%) Calc. for $C_{21}H_{25}Cl_2NOPtS$ (found): C, 38.14(38.0); H, 3.81(3.75) and N, 2.12(2.02). MS(FAB$^+$): m/z = 625.5{[M]-Cl]}$^+$. IR: ν (>C=N–) = 1614 cm^{-1}. [α]$_D$ (298 K) (c = 0.06 g/100 mL) = +386. ^{1}H-NMR data (in $CDCl_3$): δ = 1.99[d, 6H, $^3J_{H,H}$ = 6.8, Me]; 3.40[s, 6H, $^3J_{Pt,H}$ = 19, Me(dmso)]; 4.17(s, 5H, C_5H_5); 4.56(s,1H, H^4); 4.68(s, H, H^3); 4.99(s, 1H, H^2); 5.46(m, 1H, >CH-), 6.05(s, 1H, H^5); 7.36–7.50 (br.,3H, $H^{3'}$, $H^{4'}$ and $H^{5'}$); 7.63(d, 1H, $^3J_{H,H}$ = 7.5, $H^{2'}$) and 7.86 (s, 1H, $^3J_{Pt,H}$ = 87, –CH=N–). ^{1}H-NMR data (in CD_3CN): δ = 2.02 (d, 6H, Me) [83]; 3.38[s, 6H, $^3J_{Pt,H}$ = 18, Me(dmso)]; 4.20(s, 5H, C_5H_5); 4.55(s,1H, H^4); 4.66(s, H, H^3); 4.70(s, 1H, H^5); 5.53(m, 1H, >CH–), 6.15(s, 1H, H^2); 7.41–7.54 (br.,3H, $H^{3'}$, H4' and $H^{5'}$); 7.70(d, 1H, $^3J_{H,H}$ = 7.5, $H^{2'}$) and 7.88 (s, 1H, $^3J_{Pt,H}$ = 86, –CH=N–). ^{13}C{^{1}H}NMR data (in $CDCl_3$): δ = 20.8 (Me), 43.7 [Me(dmso)], 69.5 (>CH–), 70.1 (C_5H_5), 71.8 (C^2), 71.5 (C^5), 73.6 (C^4), 73.8 (C^2), 74.3 (C^1), 128.9 ($C^{2'}$ and $C^{6'}$), 128.7($C^{4'}$), 129.1($C^{3'}$ and $C^{5'}$), 139.8($C^{1'}$) and 169.3(–CH=N–). ^{195}Pt{^{1}H }-NMR data: δ = −2934 ppm.

Figure A1. Atom labelling scheme for compound **2a**.

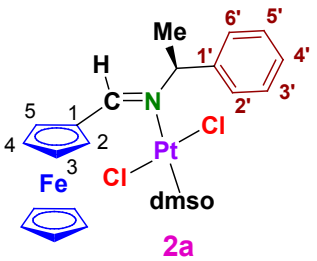

Figure A2. Atom labelling scheme for compound **7a**.

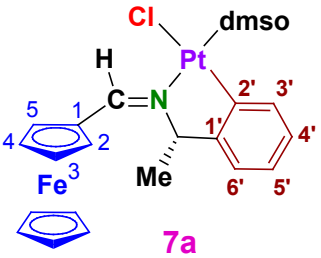

Figure A3. Atom labelling scheme for diastereomers **8a** and **9a**.

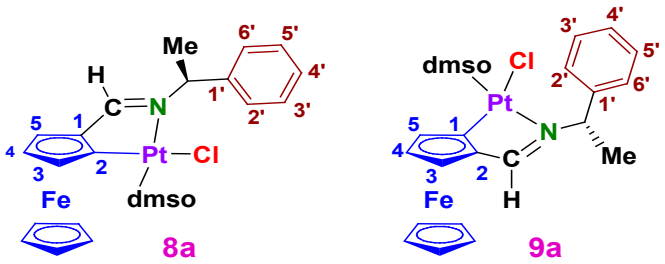

Figure A4. Atom labelling scheme for compound **7b**.

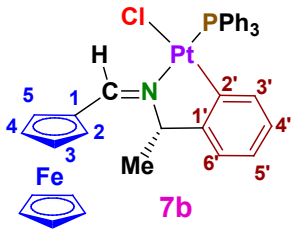

Figure A5. Atom labelling scheme for compound **8b**.

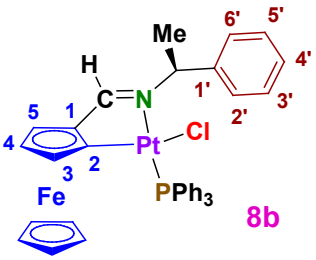

Figure A6. Atom labelling scheme for compound **9b**.

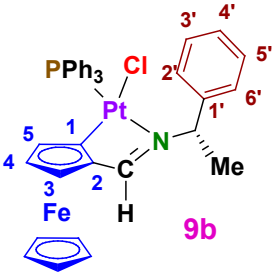

*A2.2. (S$_C$)-[Pt{κ^2-C,N[(C$_6$H$_4$)CH(Me)–N=C(H)Fc]}Cl(dmso)] (**7a**)*

Anal. (%) Calc. for $C_{21}H_{24}ClFeNOPtS$ (found): C, 40.36 (40.4); H, 3.87 (3.95), N, 2.24 (2.2) and S, 4.85 (4.9). MS(FAB$^+$): *m*/*z* = 589.1 {[M]-Cl}$^+$. IR: *ν* (>C=N–) = 1614 cm^{-1}. [α]$_D$ (298 K) (*c* = 0.03 g/100 mL) = +842. ^{1}H-NMR data (in $CDCl_3$): δ = 1.79 (d, 6H, $^3J_{H,H}$ =6.9, Me), 3.61 [s, 3H, $^3J_{Pt–H}$ = 19, Me(dmso)], 3.61[s, 3H, $^3J_{Pt–H}$ = 19, Me(dmso)], 4.38 (s, 5H, C_5H_5), 4.65 (s, 1H, H^4), 4.69 (s, 1H, H^3), 4.72 (s, 1H, H^2), 4.78(s. 1H, H^5), 5.18 (m, 1H, >CH–), 6.90–7.20 (br.m, 3H, H$^{4'}$ H$^{5'}$ H$^{6'}$), 8.2 (d, 1H, $^3J_{H,H}$ = 7.5, H$^{3'}$), and 8.91 (s, 1H, $^3J_{Pt–H}$ = 55, –CH=N–). ^{1}H-NMR data (in CD_3CN): δ = 1.81 (d, 6H, $^3J_{H,H}$ = 7.6, Me), 3.62 (br.s, 6H, Me(dmso)), 4.40 (s, 5H, C_5H_5), 4.67 (s, 1H, H^4), 4.70 (s, 1H, H^3), 4.74 (s, 1H, H^2), 4.8 (s. 1H, H^5), 5.15 (m, 1H, >CH–), 6.85–7.20 (br.m, 3H, H$^{4'}$ H$^{5'}$ H$^{6'}$), 8.2 (d 1H, $^3J_{H,H}$ = 7.2, H$^{6''}$), and 8.90 (s, 1H, $^3J_{Pt–H}$ = 57, –CH=N–). ^{13}C{^{1}H}-NMR data (in $CDCl_3$): δ = 25.6 (Me); 47.2 and 50.4 (Me(dmso)), 70.4 (>CH–); 71.6 (C_5H_5); 72.8 (C^1); 75.2 (C^3 and C^4); 76.4 (C^2 and C^5); 127.2 (C$^{6'}$); 126.0 (C$^{3'}$); 127.2 (C$^{4'}$); 136.5 (C$^{5'}$); 156.0 (C$^{2'}$); and 177.6(–CH=N). ^{195}Pt{^{1}H}-NMR data: δ = −3610 ppm.

*A2.3. The mixture (**II**) of the Two Diastereomers of [Pt{{κ^2-C,N[(η^5-C$_5$H$_3$)–CH=N–{CH(Me)(C$_6$H$_5$)}] Fe(η^5-C$_5$H$_5$)}Cl(dmso)] (**8a** and **9a**)*

Anal. (%) Calc. for $C_{21}H_{24}ClFeNOPtS$ (found): C, 40.36 (40.25); H, 3.87 (4.0), N, 2.24 (2.30) and S, 4.85 (4.67). MS(FAB$^+$): *m*/*z* = 587 {[M]-Cl}$^+$. IR: *ν* (>C=N–) = 1593 cm^{-1} (broad). ^{1}H-NMR data (in $CDCl_3$) for (**8a**) (minor component): δ = 1.84 (d, 6H, $^3J_{H,H}$ = 6.5, Me), 3.18 (s, 6H, $^3J_{Pt,H}$ = 18.4, Me(dmso)). 4.36 (s, 5H, C_5H_5), 4.66 (s, 1H, H^3), 4.68 (s, H, H^3), 4.80 (s, 1H, H^5), 5.42 (m, 1H, >CH–), 7.15–7.52 (br. m.3H, H$^{3'}$, H$^{4'}$ and H$^{5'}$), 7.62 (d, 2H, $^3J_{H,H}$ = 7.2, H$^{6'}$) and 8.22 (s, 1H, $^3J_{Pt,H}$ = 102, –CH=N–). For **9a**: (major component): δ = 1.97 (d, 6H, Me), 3.18 (s, 6H, $^3J_{Pt,H}$ = 18.5, Me(dmso)), 4.21 (s, 5H, C_5H_5), 4.43 (s, 1H, H^4), 4.54 (s, H, H^3), 4.76 (s, 1H, H^5), 5.38 (br.m, 1H, >CH–), 7.15–7.52 (br. m., 3H, H$^{3'}$, H$^{4'}$ and H$^{5'}$), 7.7 (d, 2H, $^3J_{H,H}$ = 7.2, H$^{6'}$) and 7.90 (s, 1H, $^3J_{Pt,H}$ = 97, –CH=N–).

*A2.4. (S$_C$)-[Pt{κ^2-C,N[(C$_6$H$_4$)CH(Me)–N=C(H)Fc]}Cl(PPh$_3$)] (**7b**)*

Anal. (%) Calc. for $C_{37}H_{33}ClFeNPPt$ (found): C, 54.93 (55.05); H, 4.11 (4.15) and N, 1.73 (1.8). MS (FAB$^+$): *m*/*z* = 808 [M]$^+$ and 772 {[M]-Cl}$^+$. IR: ν (>C=N–) = 1603 cm^{-1}. [α]$_D$ (298 K) (*c* = 0.02 g/100 mL) = +896.

^{1}H-NMR data (in $CDCl_3$): δ = 1.90 (d, 3H, $^3J_{H,H}$ = 7.2, Me), 4.32 (s, 5H, C_5H_5), 4.57 (s, H, H^3), 4.65 (br, 2H, H^2 and H^4), 4.78 (br. 1H, H^5), 5.36 (m, 1H, >CH–), 6.35 (br.d, $^3J_{H,H}$ ≈ 7.6, 1H, H$^{4'}$), 6.52(dd, 1H, $^3J_{H,H}$ = 7.5, $^4J_{P,H}$ = 5.1, H$^{3'}$), 6.84 (t, $^3J_{H,H}$ = 7.5,1H, H$^{5'}$), 6.98 (d, 1H, $^3J_{H,H}$ = 7.3, H$^{6'}$), 7.29–7.90 (m, 15H, aromatic protons of PPh_3) and 9.17 (d, 1H. $^3J_{Pt,H}$ = 51.2 and $^4J_{P,H}$ = 77, –CH=N–). ^{1}H-NMR data (in CD_3CN): δ = 1.94 (d, 3H, $^3J_{H,H}$ = 7.2, Me), 4.32 (s, 5H, C_5H_5), 4.60 (s, H, H^3), 4.65 (br., 2H, H^2 and H^4), 4.81 (br. 1H, H^5), 5.40 (m, 1H, >CH–), 6.37 (br.d, 1H, $^3J_{H,H}$ ≈ 7.6, $^4J_{P,H}$ = 6.2, H$^{4'}$), 6.52(m, 1H, H$^{3'}$), 6.84 (br.t, 1H, H$^{5'}$), 6.98 (d, 1H, H$^{6'}$), 7.29–7.90 (m, 16H, aromatic prótons of PPh_3) and 9.17 (d, 1H. $^3J_{Pt,H}$ = 51.2 and $^4J_{P,H}$ = 8.5, –CH=N–). ^{13}C{^{1}H}-NMR data (in $CDCl_3$): δ = 26.1(Me), 69.0(C^5), 70.5 (C_5H_5), 70.9 (>CH–), 72.3 (C^2), 73.5 (C^3), 73.2 (C^1); 73.5 (C^4), 75.1 (C^2); 125.1 (C$^{4'}$), 125.3 (C$^{5'}$), 135.6 (C$^{6'}$), 138.2 (C$^{1'}$), 148.1 (C$^{2'}$), 166.0 (–CH=N–) and four additional doublets centred

at 128.0, 130.6; 131.1 and 135.0 due to the carbon-13 nuclei of the PPh_3 ligand. $^{31}P\{^1H\}$-NMR data: δ = 19.1 ($^1J_{Pt-P}$= 3801)]. $^{195}Pt\{^1H\}$-NMR data δ = −3965 ppm ($^1J_{P,Pt}$ = 3800).

*A2.5. Diastereomers of [Pt{κ²-C,N[(η⁵-C₅H₃)-CH=N-CH(Me)(C₆H₅)]Fe(η⁵-C₅H₅)}Cl(PPh₃)] (**8b** and **9b**)*

For **8b**: Anal. (%) Calc. for $C_{37}H_{33}ClFeNPPt$ (found): C, 54.93(54.80); H, 4.11(4.15.) and N, 1.73 (1.6). MS (FAB^+): *m/z* = 773.5 $\{[M]-Cl\}^+$. IR: *ν* (>C=N–) = 1595 cm^{-1} $[\alpha]_D$ (298 K) (*c* = 0.04 g/100 mL) = −2016.^{1}H-NMR data for **8b** (in $CDCl_3$) δ = 1.85 (d, 3H, $^3J_{H,H}$ = 7, Me), 3.84 (s, 5H, C_5H_5), 3.25 (s, H, H^3), 4.41 (s, 1H, H^4), 4.57 (br. 1H, H^5), 6.20 (m, 1H, >CH–), 7.30–7.80 (br.m, 20H, $H^{2'}$–$H^{6'}$ and PPh_3) and 8.14 (d, 1H. –CH=N–,$^4J_{P,H}$= 8 and $^3J_{Pt,H}$ = 90). ^{1}H-NMR data for **8b** (in CD_3CN): δ = 1.92 (d, 3H, $^3J_{H,H}$ = 7, Me), 3.92 (s, 5H, C_5H_5), 3.35 (s, H, H^3), 4.42 (s, 1H, H^4), 4.55 (br. 1H, H^5), 6.18 (m, 1H, >CH–), 7.30–7.86 (br.m, 20H, $H^{2'}$–$H^{6'}$ and PPh_3) and 8.15 (d, 1H. –CH=N–, $^4J_{P,H}$ = 8 and $^3J_{Pt,H}$ = 90). $^{13}C\{^1H\}$NMR data (in $CDCl_3$): δ = 20.8 (Me), 69.5 (>CH–), 70.1 (C_5H_5), 71.8 (C^2), 71.5 (C^5), 73.6 (C^4), 73.8 (C^2), 74.3 (C^1), 128.9 ($C^{2'}$ and $C^{6'}$), 128.7 ($C^{4'}$), 129.1 ($C^{3'}$ and $C^{5'}$), 139.8 ($C^{1'}$), 169.3 (–CH=N–) and four additional doublets centred at ca. 128.0, 130.6; 131.1 and 135.0 ppm due to the carbon-13 nuclei of the PPh_3 ligand. $^{31}P\{^1H\}$-NMR data: δ = 15.9 ($^1J_{Pt,P}$ = 4191). $^{195}Pt\{^1H\}$-NMR data δ = −4176 ($^1J_{P,Pt}$ = 4190).

For **9b**: Anal. (%) Calc. for $C_{37}H_{33}ClFeNPPt$ (found): C, 54.93 (54.80); H, 4.11 (4.15.) and N, 1.73 (1.6). MS (FAB^+): *m/z* = 773.1$\{[M]-Cl\}^+$. IR: *ν*(>C=N–) = 1595 cm^{-1}. $[\alpha]_D$ (298 K) (*c* = 0.04 g/100 mL) = +1577. ^{1}H-NMR data for **9b** (in $CDCl_3$): δ =1.92 (d, 3H, $^3J_{H,H}$ = 7, Me), 3.57 (s, 5H, C_5H_5), 3.28 (s, H, H^3), 4.55 (s, 1H, H^4), 4.61 (br. 1H, H^5), 6.40 (m, 1H, >CH-), 7.30–7.80 (br.m, 20H, $H^{2'}$–$H^{6'}$ and PPh_3) and 8.08 (d, 1H. –CH=N–,$^4J_{P,H}$ = 8.0 and $^3J_{Pt,H}$ = 94). ^{1}H-NMR data for **9b** (in CD_3CN): δ = 1.99 (d, 3H, $^3J_{H,H}$ = 7, Me) [83] 3.617 (s, 5H, C_5H_5), 3.40 (s, H, H^3), 4.60 (s, 1H, H^4), 4.61 (br. 1H, H^5), 6.41 (m, 1H, >CH–), 7.29–7.82 (br.m, 20H, $H^{2'}$–$H^{6'}$ and PPh_3) and 8.10 (d, 1H. –CH=N–, $^4J_{P,H}$ = 7.8 and $^3J_{Pt,H}$ = 90). $^{13}C\{^1H\}$NMR data (in $CDCl_3$): δ = 21.2(Me), 68.5(>CH–), 70.8 (C_5H_5),73.6 (C^3), 74.8 (C^5), 88.16 (C^1), 92.2 (C^2), 73.8 (C^4), 128.6 ($C^{2'}$ and $C^{6'}$), 128.3 ($C^{4'}$), 129.1 ($C^{3'}$ and $C^{5'}$), 138.9 ($C^{1'}$), 180.1 (–CH=N–) and four additional doublets centred at 128.0, 130.6; 131.1 and 135.0 due to the carbon-13 nuclei of the PPh_3 ligand. $^{31}P\{^1H\}$-NMR data: δ = 16.2 ($^1J_{Pt,P}$ = 4202). $^{195}Pt\{^1H\}$-NMR data:δ = −4192 ($^1J_{Pt,P}$ = 4202).

Conflicts of Interest

The authors declare no conflict of interest.

References and Notes

1. Crespo, M. Effect of fluorine substituents in intramolecular activation of carbon-fluorine and carbon-hydrogen bonds by platinum(II). *Organometallics* **2012**, *31*, 1216–1234.
2. Guerchais, V.; Ordronneau, L.; le Bozec, H. Recent developments in the field of metal complexes containing photochromic ligands: Modulation of linear and nonlinear optical properties. *Coord. Chem. Rev*. **2010**, *254*, 2533–2545.

3. Diez, A.; Lalinde, E.; Moreno, M.T. Heteropolynuclear cycloplatinated complexes: Structural and photophysical properties. *Coord. Chem. Rev.* **2011**, *255*, 2426–2477.
4. Kalinowski, J.; Fattori, V.; Cocchi, M.; Williams, J.A.G. Light-emitting devices based on organometallic platinum complexes as emitters. *Coord. Chem. Rev.* **2011**, *255*, 2401–2425.
5. Williams, J.A.G.; Develay, S.; Rochester, D.L.; Murphy, L. Optimising the luminescence of platinum(II) complexes and their application in organic light emitting devices (OLEDs). *Coord. Chem. Rev*. **2008**, *252*, 2596–2611.
6. Siu, P.K.-M.; Ma, D.-L.; Che, C.-M. Luminescent cyclometalated platinum(II) complexes with amino acid ligands for protein binding. *Chem. Commun*. **2005**, 1025–1027.
7. Sicilia, V.; Fuertes, S.; Martin, A.; Palacios, A. *N*-Assisted C_{Ph}−H Activation in 3,8-dinitro-6-phenylphenanthridine. New *C*,*N*-cyclometalated compounds of platinum(II): Synthesis, structure, and luminescence studies. *Organometallics* **2013**, *32*, 4092–4102.
8. Hudson, Z.M.; Sun, C.; Helander, M.G.; Amarne, H.; Lu, Z.-H.; Wang, S. Enhancing Phosphorescence and Electrophosphorescence Efficiency of Cyclometalated Pt(II) Compounds with Triarylboron. *Adv. Funct. Mat*. **2010**, *20*, 3426–3439.
9. Rausch, A.F.; Murphy, L.; Williams, J.A.G.; Yersin, H. Improving the Performance of Pt(II) Complexes for Blue Light Emission by Enhancing the Molecular Rigidity. *Inorg. Chem.* **2012**, *51*, 312–319.
10. Gandioso, A.; Valle-Sistac, J.; Rodriguez, L.; Crespo, M.; Font-Bardia, M. Platinum(II) Compounds Containing Cyclometalated Tridentate Ligands: Synthesis, Luminescence Studies, and a Selective Fluoro for Methoxy Substitution. *Organometallics* **2014**, *33*, 561–570.
11. Arias, A.; Forniés, J.; Fortuño, C.; Martin, A.; Latronico, M.; Mastrorilli, P.; Todisco, S.; Gallo, V. Formation of P–C Bond through Reductive Coupling between Bridging Phosphido and Benzoquinolinate Groups. Isolation of Complexes of the Pt(II)/Pt(IV)/Pt(II) Sequence. *Inorg. Chem*. **2012**, *51*, 12682–12696.
12. Liu, F.; Pullarkat, S.A.; Tan, K.-W.; Li, Y.; Leung, P.-H. Enantioselective Diels-Alder Reaction of 3-Diphenylphosphinofuran with 1-Phenyl-3,4-dimethylphosphole and Subsequent Synthetic Manipulations of the Cycloadduct. *Organometallics* **2009**, *28*, 6254–6259.
13. Newman, C.P.; Casey-Green, K.; Clarkson, G.J.; Cave, G.W.V.; Errington, W.; Rourke, J.P. Cyclometallated platinum(II) complexes: oxidation to, and C–H activation by platinum(IV). *Dalton Trans*. **2007**, *29*, 3170–3182.
14. Berenguer, J.R.; Fernández, J.; Giménez, N.; Lalinde, E.; Moreno, M.T.; Sánchez, S. Unexpected Formation of Ferrocenyl(vinyl)benzoquinoline Ligands by Oxidation of an Alkyne Benzoquinolate Platinum(II) Complex. *Organometallics* **2013**, *32*, 3943–3953.
15. Xiao, X.-S.; Kwong, W.-L.; Guan, X.; Yang, C.; Lu, W.; Che, C.-M. Platinum(II) and Gold(III) Allenylidene Complexes: Phosphorescence, Self-Assembled Nanostructures and Cytotoxicity. *Chem.-Eur. J.* **2013**, *19*, 9457–9462.
16. Li, K.; Chen, Y.; Lu, W.; Zhu, N.; Che, C.M. A Cyclometalated Platinum(II) Complex with a Pendent Pyridyl Motif as Solid-State Luminescent Sensor for Acidic Vapors. *Chem.-Eur. J.* **2011**, *17*, 4109–4112.

17. Suntharalingam, K.; Łęczkowska, A.; Furrer, M.A.; Wu, Y.; Kuimova, K.K.; Therrien, B.; White, A.J.P.; Vilar, R. A Cyclometallated Platinum Complex as a Selective Optical Switch for Quadruplex DNA. *Chem.-Eur. J.* **2012**, *18*, 16277–16282.
18. Boixel, J.; Guerchais, V.; le Bozec, H.; Jacquemin, D.; Amar, A.; Boucekkine, A.; Colombo, A.; Dragonetti, C.; Marinotto, D.; Roberto, D.; *et al.* Second-Order NLO Switches from Molecules to Polymer Films Based on Photochromic Cyclometalated Platinum(II) Complexes. *J. Am. Chem. Soc*. **2014**, *136*, 5367–5375.
19. Koo, C.-K.; Lam, B.; Leung, S.-K.; Lam, M.H.-W.; Wong, W.-Y. A "Molecular Pivot-Hinge" Based on the pH-Regulated Intramolecular Switching of Pt–Pt and π–π Interactions. *J. Am. Chem. Soc*. **2006**, *128*, 16434–16435.
20. Pérez, S.; López, C.; Caubet, A.; Solans, X.; Font-Bardía, M. New Heterodimetallic Platinum(II) Complexes Potentially Useful as Molecular Switches. *Eur. J. Inorg. Chem.* **2008**, 1599–1612.
21. Ho, Y.-M.; Au, N.-P.B.; Wong, K.-L.; Chan, C.T.-L.; Kwok, W.-M.; Law, G.-L.; Tang, K.-K.; Wong, W.-Y.; Ma, C.-H.E.; Lam, M.H.-W. A lysosome-specific two-photon phosphorescent binuclear cyclometalated platinum(II) probe for in vivo imaging of live neurons. *Chem. Commun*. **2014**, *50*, 4161–4163.
22. Cocchi, M.; Kalinowski, J.; Fattori, V.; Williams, J.G.; Murphy, L. Control of magnetic-field effect on electro-luminescence in Alq3-based organic light emitting diodes. *Appl. Phys. Lett*. **2009**, *94*, 166104.
23. Zou, T.; Liu, J.; Lum, C.T.; Ma, C.; Chan, R.C.T.; Lok, C.-N.; Kwok, W.-M.; Che, C.-M. Luminescent Cyclometalated Platinum(II) Complex Forms Emissive Intercalating Adducts with Double-Stranded DNA and RNA: Differential Emissions and Anticancer Activities. *Angew. Chem. Int. Ed*. **2014**, *53*, 10119–10123.
24. Kalinowski, J.; Cocchi, M.; Virgili, D.; Fattori, V.; Williams, J.G. Mixing of Excimer and Exciplex Emission: A New Way to Improve White Light Emitting Organic Electrophosphorescent Diodes. *Adv. Mater.* **2007**, *19*, 4000−4005.
25. Yu, J.; Luo, J.; Chen, Q.; He, K.; Meng, F.; Deng, X.; Wang, Y.; Tan, H.; Jiang, H.; Zhu, W. Synthesis and optoelectronic properties of a novel dinuclear cyclometalated platinum(II) complex containing triphenylamine-substituted indolo[3,2-b]carbazole derivative in the single-emissive-layer WPLEDs. *Tetrahedron* **2014**, *70*, 1246–1251.
26. Escolà, A.; Crespo, M.; Quirante, J.; Cortés, R.; Jayaraman, A.; Badia, J.; Baldomà, L.; Calvet, T.; Font-Bardia, M.; Cascante, M. Exploring the Scope of $[Pt_2(4\text{-}FC_6H_4)_4(\mu\text{-}SEt_2)_2]$ as a Precursor for New Organometallic Platinum(II) and Platinum(IV) Antitumor Agents. *Organometallics* **2014**, *33*, 1740–1750.
27. Cutillas, N.; Martínez, A.; Yellol, G.S.; Rodríguez, V.; Zamora, A.; Pedreño, M.; Donaire, A.; Janiak, C.; Ruiz, J. Anticancer *C*,*N*-Cycloplatinated(II) Complexes Containing Fluorinated Phosphine Ligands: Synthesis, Structural Characterization, and Biological Activity. *Inorg. Chem*. **2013**, *52*, 13529–13535.
28. Ruíz, J.; Vicente, C.; de Haro, C.; Espinosa, A. Synthesis and Antiproliferative Activity of a *C*,*N*-Cycloplatinated(II) Complex with a Potentially Intercalative Anthraquinone Pendant. *Inorg. Chem.* **2011**, *50*, 2151−2158.

29. Cortés, R.; Crespo, M.; Davin, L.; Martin, R.; Quirante, J.; Ruiz, D.; Messeguer, R.; Calvis, C.; Baldomà, L.; Badia, J.; *et al.* Cyclopalladated primary amines: A preliminary study of antiproliferative activity through apoptosis induction. *Eur. J. Med. Chem*. **2012**, *54*, 557–566.
30. Quirante, J.; Ruíz, D.; González, A.; López, C.; Cascante, M.; Cortés, R.; Messeguer, R.; Calvis, C.; Baldomà, L.; Pascual, A.; *et al.* Platinum(II) and palladium(II) complexes with (N,N′) and (C,N,N′)$^{-}$ ligands derived from pyrazole as anticancer and antimalarial agents: Synthesis, characterization and in vitro activities. *Inorg. Biochem*. **2011**, *105*, 1720–1728.
31. Ruíz, J.; Rodriguez, V.; Cutillas, N.; Espinosa, A.; Hannon, M. Novel *C*,*N*-chelate platinum(II) antitumor complexes bearing a lipophilic ethisterone pendant. *J. Inorg. Biochem*. **2011**, *105*, 525–531.
32. Albert, J.; Bosque, R.; Crespo, M.; Granell, J.; López, C.; Cortés, R.; Gonzalez, A.; Quirante, J.; Calvis, C.; Messeguer, R.; *et al.* Pt(II) complexes with (*N*,*N*') or (C,N,E)$^{-}$ (*E* = N,S) ligands: Cytotoxic studies, effect on DNA tertiary structure and structure–activity relationships. *Bioorg. Med. Chem.* **2013**, *21*, 4210–4217.
33. Frik, M.; Jiménez, J.; Vasilevski, V.; Carreira, M.; de Almeida, A.; Benoit, F.; Gascón, E.; Sanaú, M.; Casini, A.; Contel, M. Luminescent iminophosphorane gold, palladium and platinum complexes as potential anticancer agents. *Inorg. Chem. Front.* **2014**, *1*, 231–241.
34. Togni, A.; Hayashi, T. *Ferrocenes. Homogeneous Catalysis, Organic Synthesis. Materials Science*; VCH: Weinheim, Germany, 1995.
35. Stepnicka, P. *Ferrocene. Ligands, Materials and Biomolecules*; Wiley: Weinheim, Germany, 2008.
36. López, C.; González, A.; Bosque, R.; Basu, P.K.; Font-Bardia, M.; Calvet, M.T. Platinum(II) and palladium(II) complexes derived from 1-ferrocenylmethyl-3,5-diphenylpyrazole. Coordination, cyclometallation or transannulation? *RSC Adv.* **2012**, *2*, 1986–2002.
37. Wu, Y.; Huo, S.; Gong, J.; Cui, X.; Ding, L.; Ding, K.; Du, C.; Liu, Y.; Song, M. Studies on the cyclometallation of ferrocenylimines. *J. Organomet. Chem.* **2001**, *637–639*, 27–48.
38. Dai, L.-X.; Hou, X. *Chiral Ferrocenes in Asymmetric Catalysis*; Wiley: Weinheim, Germany, 2010.
39. Weiss, M.; Frey, W.; Peters, R. Asymmetric Synthesis of Heterobimetallic Planar Chiral Ferrocene Pallada-/Platinacycles and Their Application to Enantioselective Aza-Claisen Rearrangements. *Organometallics* **2012**, *31*, 6365–6372.
40. López, C.; Caubet, A.; Pérez, S.; Solans, X.; Font-Bardia, M. Easy access to diastereomerically pure platinacycles. *Chem. Commun*. **2004**, 540–541.
41. López, C.; Caubet, A.; Pérez, S.; Solans, X.; Font-Bardía, M.; Molins, M. Chiral Platinum(II) Compounds Containing Ferrocenyl Schiff Bases Acting as (N), (N,O)$^{-}$, [C(sp^2,ferrocene),N]$^{-}$ or [C(sp^2,ferrocene),N,O]$^{2-}$ Ligands. *Eur. J. Inorg. Chem.* **2006**, 3974–3984.
42. Talancón, D.; López, C.; Font-Bardía, M.; Calvet, T.; Quirante, J.; Calvis, C.; Messeguer, R.; Cortés, R.; Cascante, M.; Baldomà, L.; *et al.* Diastereomerically pure platinum(II) complexes as antitumoral agents. The influence of the mode of binding {(N), (N,O)$^{-}$ or (C,N)$^{-}$} of (1*S*,2*R*)-[(η^5-C_5H_5)Fe{(η^5-C_5H_4)\CH=N–CH(Me)–CH(OH)\C_6H_5}] and the arrangement of the auxiliary ligands. *J. Inorg. Biochem.* **2013**, *118*, 1–12.

43. Cortés, R.; Tarrado-Castellarnau, M.; Talancón, D.; López, C.; Link, W.; Ruiz, D.; Centelles, J.; Quirante, J.; Cascante, M. A novel cyclometallated Pt(II)–ferrocene complex induces nuclear FOXO3a localization and apoptosis and synergizes with cisplatin to inhibit lung cancer cell proliferation. *Metallomics* **2014**, *6*, 622–633.
44. Anderson, C.; Crespo, M.; Morris, J.; Tanski, J.M. Reactivity of cyclometallated platinum complexes with chiral ligands. *J. Organomet. Chem*. **2006**, *691*, 5635–5641.
45. Crespo, M.; Solans, X.; Font-Bardia, M. Cyclometallated platinum compounds with chiral imines. Crystal structure of [PtMe(2-FC_6H_3CH=N-(*S*)-CHMePh)(PPh_3)]. *Polyhedron* **1998**, *17*, 3927–3934.
46. Krylova, L.F.; Pavlushko, T.A. Diastereomers of trans isomers of Pt(II) complexes with alanime and phenylalanine. *Zhurnal Neorg. Khimii* **2003**, *48*, 1790–1800.
47. Ryabov, A.D.; Panyashkina, I.M.; Polyakov, V.A.; Fischer, A. Access to Central Carbon Chirality through Cycloplatination of 1-(2-Pyridinylthio)propanone by *cis*-[$PtCl_2$(*S*-SOMe(*p*-tolyl))]. The Crystal Structure of (S_sS_c)-[Pt{py{SCHC(O)Me}-2}Cl(SOMe(*p*-tolyl))]. *Organometallics* **2002**, *21*, 1633–1636.
48. Platero-Prats, A.E.; Pérez, S.; López, C.; Solans, X.; van Leeuwen, P.W.N.M.; van Strijdonck, G.P.F.; Freixa, Z. Palladium(II)-allyl complexes containing chiral *N*-donor ferrocenyl ligands. *J. Organomet. Chem*. **2007**, *692*, 4215–4226.
49. Zucca, A.; Cinellu, M.A.; Minghetti, G.; Stoccoro, S.; Manassero, M. Dinuclear, Tricyclometallated Platinum(II) Derivatives—Substitution Reactions and Reactivity of the Platinum–Carbon Bonds. *Eur. J. Inorg. Chem*. **2004**, 4484–4490.
50. Kui, S.C.F.; Hung, F.F.; Lai, S.-L.; Yuan, M.-Y.; Kwok, C.-C.; Low, K.-H.; Chui, S.S.-Y.; Che, C.-M. Luminescent Organoplatinum(II) Complexes with Functionalized Cyclometalated C^N^C Ligands: Structures, Photophysical Properties, and Material Applications. *Chem.-Eur. J.* **2012**, *18*, 96–109.
51. Crosby, S.H.; Clarkson, G.J.; Rourke, J.P. Reactions of a Platinum(II) Agostic Complex: Decyclometalation, Dicyclometalation, and Solvent-Switchable Formation of a Rollover Complex. *Organometallics* **2011**, *30*, 3603–3609.
52. Crosby, S.H.; Thomas, H.R.; Clarkson, G.J.; Rourke, J.P. Concerted reductive coupling of an alkyl chloride at Pt(IV). *Chem. Commun*. **2012**, *48*, 5775–5777.
53. Bernhardt, P.V.; Calvet, T.; Crespo, M.; Font-Bardía, M.; Jansat, S.; Martinez, M. New Insights in the Formation of Five- *versus* Seven-Membered Platinacycles: A Kinetico-Mechanistic Study. *Inorg. Chem.* **2013**, *52*, 474–484.
54. Calvet, T.; Crespo, M.; Font-Bardía, M.; Jansat, S.; Martinez, M. Kinetico-Mechanistic Studies on Intramolecular C–*X* Bond Activation (*X* = Br, Cl) of Amino-Imino Ligands on Pt(II) Compounds. Prevalence of a Concerted Mechanism in Nonpolar, Polar, and Ionic Liquid Media. *Organometallics* **2012**, *31*, 4367–4373.
55. Allen, F.H. The Cambridge Structural Database: A quarter of a million crystal structures and rising. *Acta Cryst. Sect. B: Struct. Sci*. **2002**, *B58*, 380–388.
56. Crespo, M.; Martin, R.; Calvet, T.; Font-Bardia, M.; Solans, X. Novel platinum(II) compounds with *N*-benzylidenebenzylamines: Synthesis, crystal structures and the effect of *cis* or *trans* geometry on cycloplatination. *Polyhedron* **2008**, *27*, 2603–2612.

57. López, R.; Bosque, R.; Solans, X.; Font-Bardía, M. Steric effects in ferrocenylketimines and Aldimines. X-ray Crystal Structure of [Fe(η^5-C_5H_5){(η^5-C_5H_4)C(C_6H_5)=N–R'}] (with R' = C_6H_4-4-CH_3 or C_6H_4-2-CH_3). *New J. Chem*. **1996**, *20*, 1285–1292.
58. López, C.; Bosque, R.; Solans, X.; Font-Bardía, M. Synthesis and Characterization of Optically Active Cyclopalladated Compounds containing Ferrocenylimines. *Tetrahedron: Asymm*. **1996**, *7*, 2527–2530.
59. Talancón, D.; López, C.; Font-Bardía, M.; Calvet, T.; Roubeau, O. Diastereomerically Pure Heterodi- and Heterotetrametallic (Pd and Pt) Compounds: A Study of the Effect Induced by the Binding Mode of a Ferrocene-Containing Ligand on Their Electrochemical Properties. *Eur. J. Inorg. Chem.* **2014**, 213–220.
60. López, C.; Bosque, R.; Sainz, D.; Solans, X.; Font-Bardia, M. A New Reagent for Chiral Recognition Containing a Five-Membered Palladacycle with a σ(Pd-Csp^2, ferrocene) Bond. *Organometallics* **1997**, *16*, 3261–3266.
61. Gmelin Handbuch der Anorganischen Chemie. Ferrocen 1. *Eisen Organische Verbindunge*; Slawisch, A., Ed.; Springer-Verlag: Heildelberg, Germany, 1974; Teil A.
62. Pregosin, P.S. Platinum-195 nuclear magnetic resonance. *Coord. Chem. Rev.* **1982**, *44*, 247–291.
63. Riera, X.; López, C.; Caubet, A.; Moreno, V.; Solans, X.; Font-Bardia, M. Platinum(II) and Palladium(II) Compounds Containing Chiral Thioimines. *Eur. J. Inorg. Chem.* **2001**, 2135–2141.
64. Shen, S.-L.; Shao, J.-H.; Luo, J.-Z.; Liu, J.-T.; Miao, J.-Y.; Zhao, B.-X. Novel chiral ferrocenylpyrazolo[1,5-a][1,4]diazepin-4-onederivatives—Synthesis, characterization and inhibition against lung cancer cells. *Eur. J. Med. Chem*. **2013**, *63*, 256–268.
65. Shen, S.-L.; Zhu, J.; Li, M.; Zhao, B.-X.; Miao, J.-Y. Synthesis of ferrocenyl pyrazole-containing chiral aminoethanol derivatives and their inhibition against A549 and H322 lung cancer cells. *Eur. J. Med. Chem*. **2012**, *54*, 287–294.
66. Joksović, M.D.; Marković, V.; Juranić, Z.D.; Stanjković, T.; Jovanović, L.S.; Damijanović, I.S.; Szécsényi, K.M.; Todorović, N.; Trifunovićc, S.; Vukiević, R.D. Synthesis, characterization and antitumor activity of novel *N*-substituted α-amino acids containing ferrocenyl pyrazole-moiety. *J. Organomet. Chem*. **2009**, *694*, 3935–3942.
67. Brown, E.R.; Sandifer, J.R. *Physical Methods in Chemistry. Electrochemical Methods*; Rossiter, B.W., Hamilton, J.H., Eds.; Wiley: New York, NY, USA, 1986; Volume 4, Chapter 4.
68. Bosque, R.; López, C.; Sales, J. Substituent effects on the electrochemical behavior of iron(II) in Schiff bases derived from ferrocene and their cyclopalladated compounds. *Inorg. Chim. Acta* **1996**, *244*, 141–145.
69. Duivenvoorden, W.C.M.; Liu, Y.; Schatte, G.; Kraatz, H.-B. Synthesis of redox-active ferrocene pyrazole conjugates and their cytotoxicity in human mammary adenocarcinoma MCF-7 cells. *Inorg. Chim. Acta* **2005**, *358*, 3183–3189.
70. Becke, A.D. Density-functional thermochemistry. III. The role of exact exchange. *J. Chem. Phys.* **1993**, *98*, 5648–5652.
71. Lee, C.; Yang, W.; Parr, R.G. Development of the Colle_Salvetti correlation energy formula into a functional of the electron density. *Phys. Rev. B* **1988**, *37*, 785–789.
72. Wadt, W.R.; Hay, P.J. *Ab initio* effective core potentials for molecular calculations. Potentials for main group elements Na to Bi. *J. Chem. Phys*. **1985**, *82*, 284–298.

73. Hay, P.J.; Wadt, W.R. *Ab initio* effective core potentials for molecular calculations. Potentials for K to Au including the outermost core orbitals. *J. Chem. Phys*. **1985**, *82*, 299–310.
74. Frisch, M.J.; Trucks, G.W.; Schlegel, H.B.; Scuseria, G.E.; Robb, M.A.; Cheeseman, J.R.; Montgomery, J.A.; Vreven, T.; Kudin, K.N.; Burant, J.C. *Gaussian 03*, Revision C.02; Gaussian, Inc.: Wallingford, CT, USA, 2004.
75. Cambridge Crystallographic Data Centre. Available online: www.ccdc.cam.ac.uk/data_request/cif (accessed on 20 June 2014).
76. Price, J.H.; Williamson, A.N.; Schramm, R.F.; Wayland, B.B. Palladium(II) and platinum(II) alkyl sulfoxide complexes. Examples of sulfur-bonded, mixed sulfur- and oxygen-bonded, and totally oxygen-bonded complexes. *Inorg. Chem*. **1972**, *11*, 1280–1284.
77. Perrin, D.D.; Armarego, W.L.F. *Purification of Laboratory Chemicals*, 4th ed.; Butterworth–Heinemann: Oxford, UK, 1996.
78. Sheldrick, G.M. *SHELXS A Computer Program for Determination of Crystal Structure*; Univerversity of Göttingen: Göttingen, Germany, 1997.
79. Sheldrick, G.M. *SHELX97 A Computer Program for Determination of Crystal Structure*; Univerversity of Göttingen: Göttingen, Germany, 1997.
80. Ibers, J.A.; Hamilton, W.C. *International Tables of X-ray Crystallography*; Kynoch Press: Birmingham, UK, 1974; Volume IV, pp. 99–100, 149.
81. Flack, H.D. On enantiomorph-polarity estimation. *Acta Cryst.* **1983**, *A39*, 876–881.
82. Givens, K.T.; Kitada, S.; Chen, A.K.; Rothschiller, J.; Lee, D.A. Proliferation of human ocular fibroblasts: An assessment of *in vitro* colorimetric assays. *Investig. Ophthalmol. Vis. Sci*. **1990**, *31*, 1856–1862.
83. This signal was partially masked by the resonance due to the residual solvent.